Lithogeochemical and Petrographic Features of the Carr Porphyry and Associated Rocks, Matheson Region, Ontario

For:

6070205 Canada Inc.

Report by:

T.J. Barrett
Ore Systems Consulting
29 Toronto St. S.
Markdale
ON N0C 1H0

Feb. 10, 2012

(updated Aug. 28, 2013)

Introduction

This report presents rock classifications and an assessment of lithological relations and alteration effects in three drill holes located along northwestern margin of the Carr porphyry. The porphyry is located about 6 km north of Matheson and 60 km east of Timmins, within a regional panel of Porcupine-age clastic sedimentary rocks (2690-2685 Ma) that are bounded to the north by the Pipestone Fault and to the south by the Porcupine-Destor Fault (Fig. 1).

Drillholes completed in the northwestern part of the Carr porphyry by various companies since 1990 are shown superimposed on a total field regional magnetic map in Figure 2, with NAD83 locations shown in Figure 3. Whole-rock analyses of samples from holes CR02-1, PMC-3 and FL-53-05 are given in Table 1, together with chemical classifications. These three holes were respectively drilled by Placer Dome in 2002, Pentland Firth in 1996, and Falconbridge in 1990.

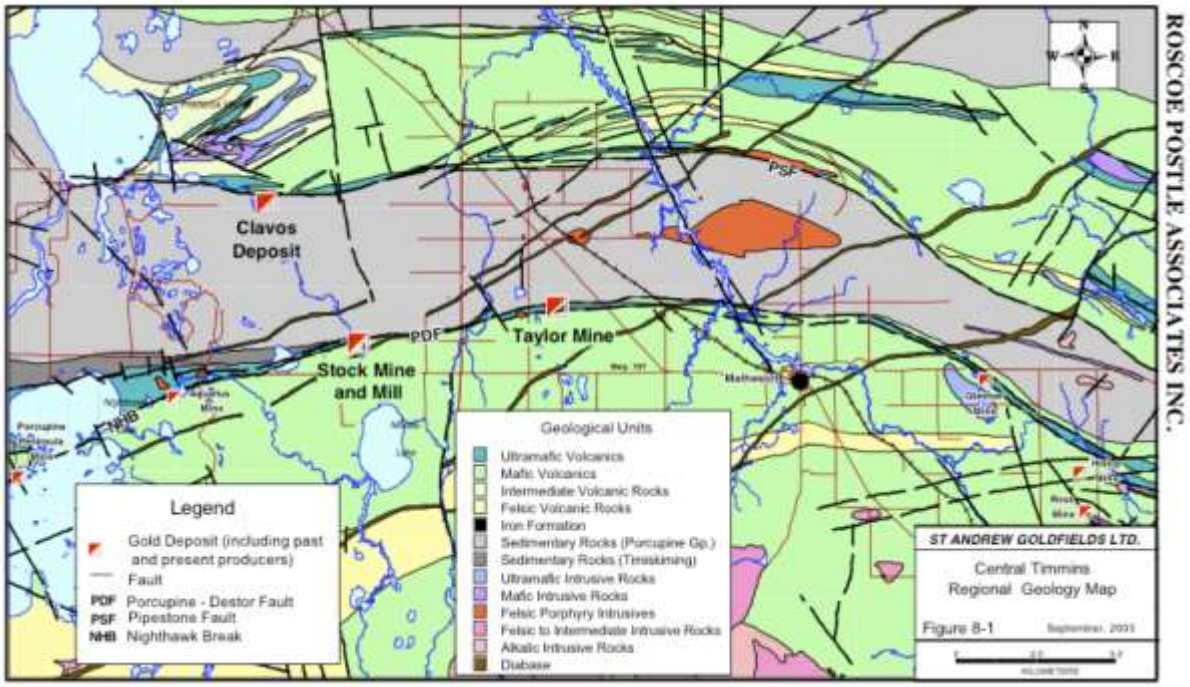

Figure 1. General geology of the eastern Abitibi greenstone belt between Nighthawk Lake - Frederick House Lake in the west, and the Hislop and Ross mines in the east (Scott Wilson RPA, 2006). The Carr porphyry is shown in red, Porcupine sedimentary rocks in grey, and older volcanic rocks in light green and yellow. PSF = Pipestone Fault; PDF = Porcupine-Destor Fault.

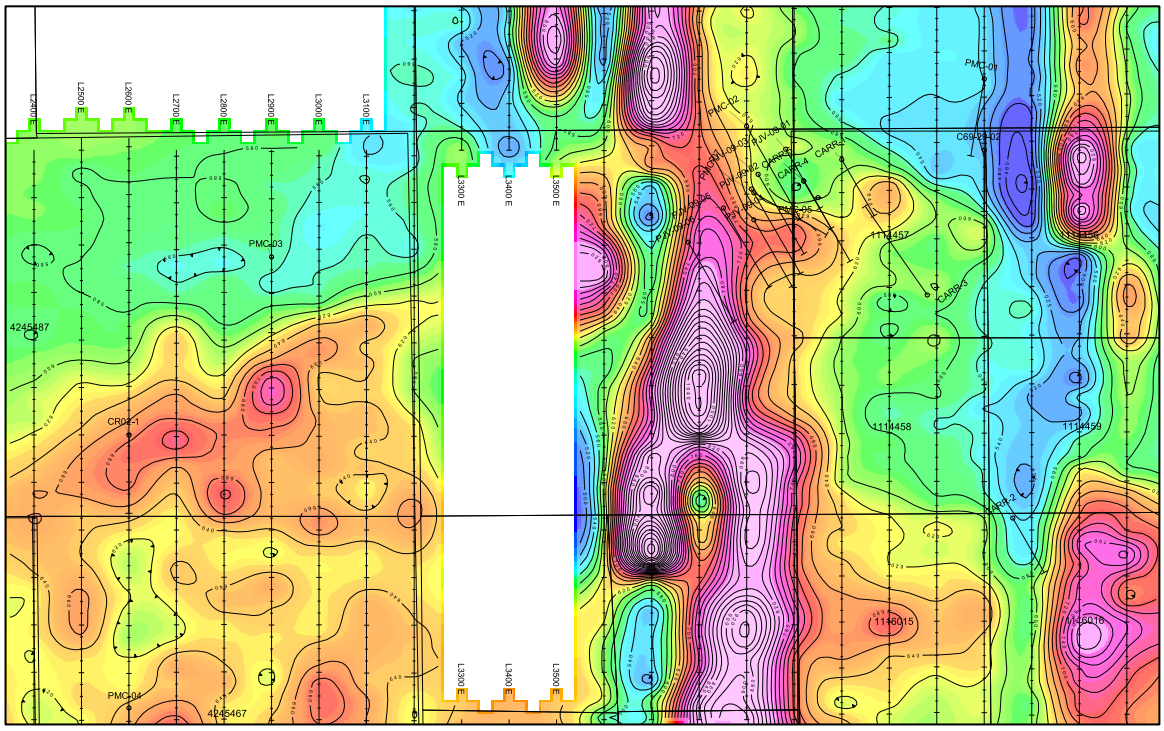

Figure 2. Total field magmatic map centred around the northern part of the Carr porphyry. Holes CR02-1 and PMC-03 lie in the western part of the map, while hole FL-53-05 (CARR-5 on the map) is located within the main cluster of holes to the northeast of centre.

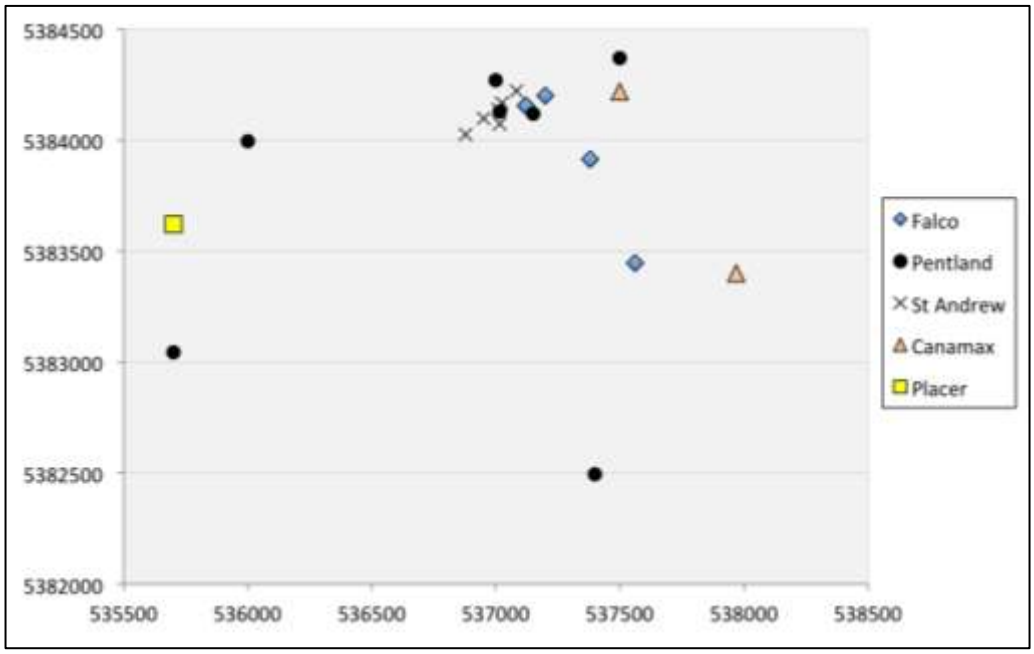

Figure 3. Locations of holes drilled in various programs since 1990. The three holes sampled in the present study are marked.

Lithogeochemistry

Methodology

Plots of one immobile-element ratio versus a second ratio, e.g., Zr/Al_2O_3 vs. Al_2O_3/TiO_2, remove the effects of alteration on the absolute abundances of individual immobile elements (Barrett and MacLean, 1999; Barrett et al., 2001, 2005). These plots, which involve both compatible and incompatible elements that are also generally immobile, can be used to identify primary rock types such as rhyolite, dacite, andesite and basalt. It is also possible to assess magmatic affinity (e.g., tholeiitic, transitional, calc-alkaline and alkaline) using the ratios of incompatible and immobile trace elements such as Zr, Nb, Y, Th and the REE. Ideally, neither fractionation nor alteration should affect the affinity ratios.

Main rock groups

Chemical analyses of the new samples from PMC-3, CR02-1 and FL-53-05 are given in Tables 1a and 1b. The former table lists the samples according to the chemical groups defined in this study, while the latter lists the samples by drill hole number and depth. Three main chemical groups have been identified on the basis of the primary chemical features of least-altered samples and the plots shown on the following pages:

1) QF porphyry of strongly calc-alkaline affinity.
2) Greywackes (including siltstones).
3) A minor “hybrid” lithology of probable mafic derivation.

Plots involving two immobile-element ratios are shown for the three groups in Figure 4. The QF porphyry and greywacke groups are well defined and separated, although each shows some internal variation, respectively due to a small amount of primary magmatic fractionation, or to sedimentary sorting effects. Rare-earth element (REE) and extended-element plots for the three chemical groups are shown in Figure 5. The composition of the Carr porphyry is compared to other porphyries in the Timmins and Kirkland Lake areas in Figure 6. Drill core and petrographic photographs and comments pertaining to holes PMC-3 and CR02-1 are given in following sections.

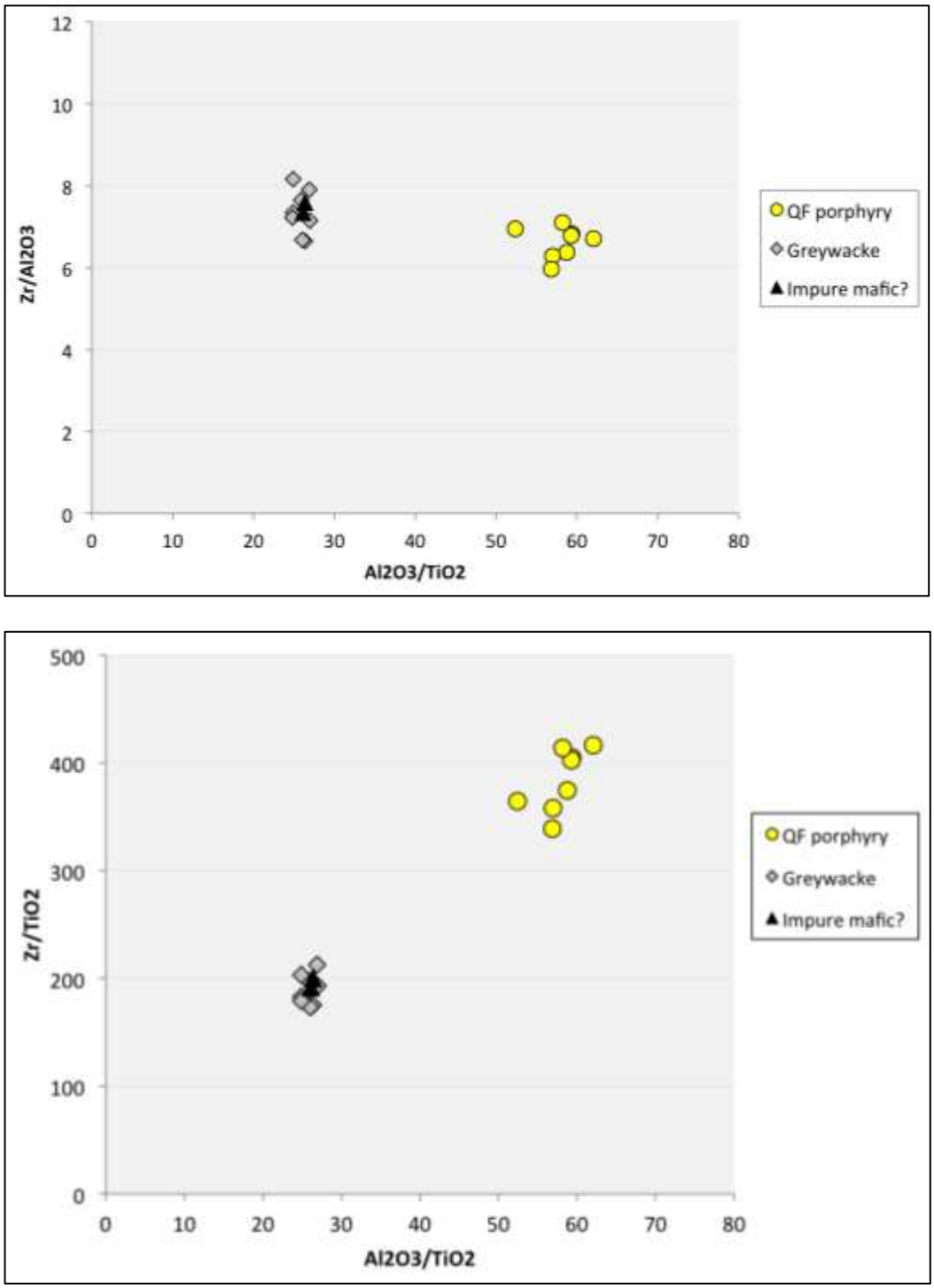

Figure 4. Immobile-element ratio plots for the Carr QF porphyry and associated rocks sampled in three drill holes. In the two above plots, the impure mafic? lithology appears identical to the greywackes. However, in the two affinity plots below, it plots in a separate, transitional field. The impure mafic? lithology contains quartz and plagioclase phenocrysts similar to those in the QF porphyry but has much higher MgO and Cr contents consistent with a mafic precursor.

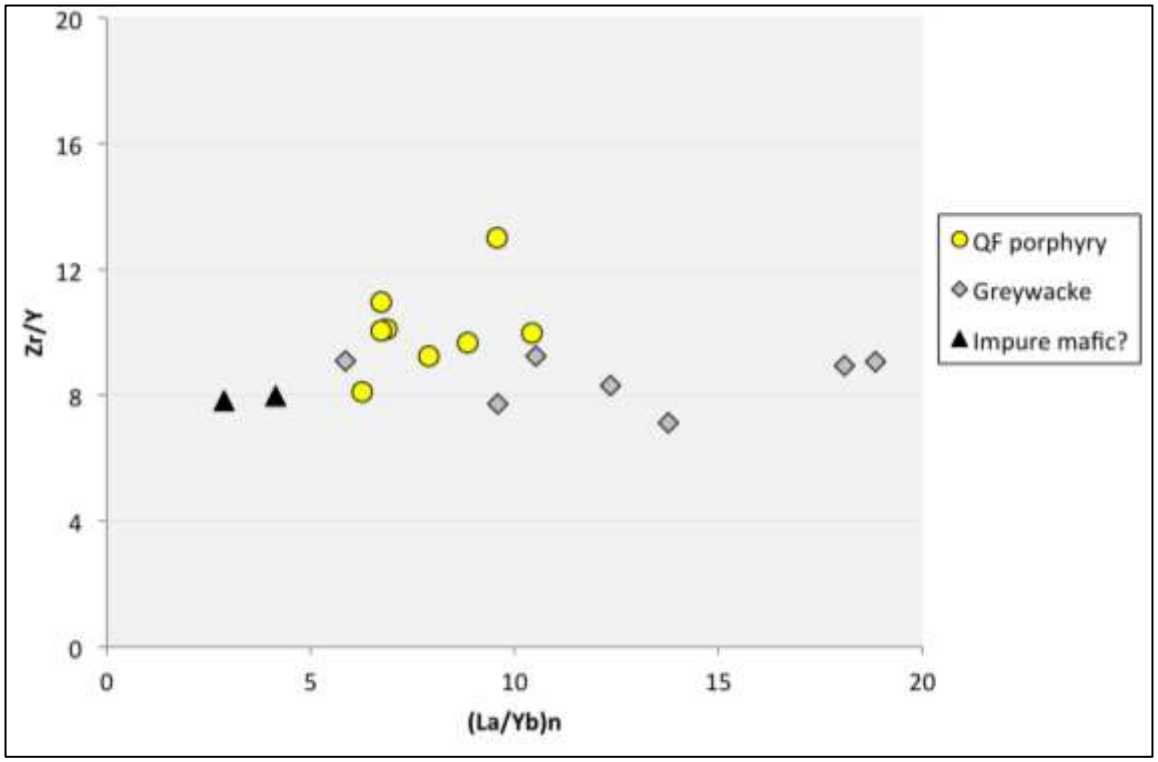
20
16
12
8
4
0
Zr/Y
0
5
10
15
20
(La/Yb)n
QF porphyry
Greywacke
Impure mafic?

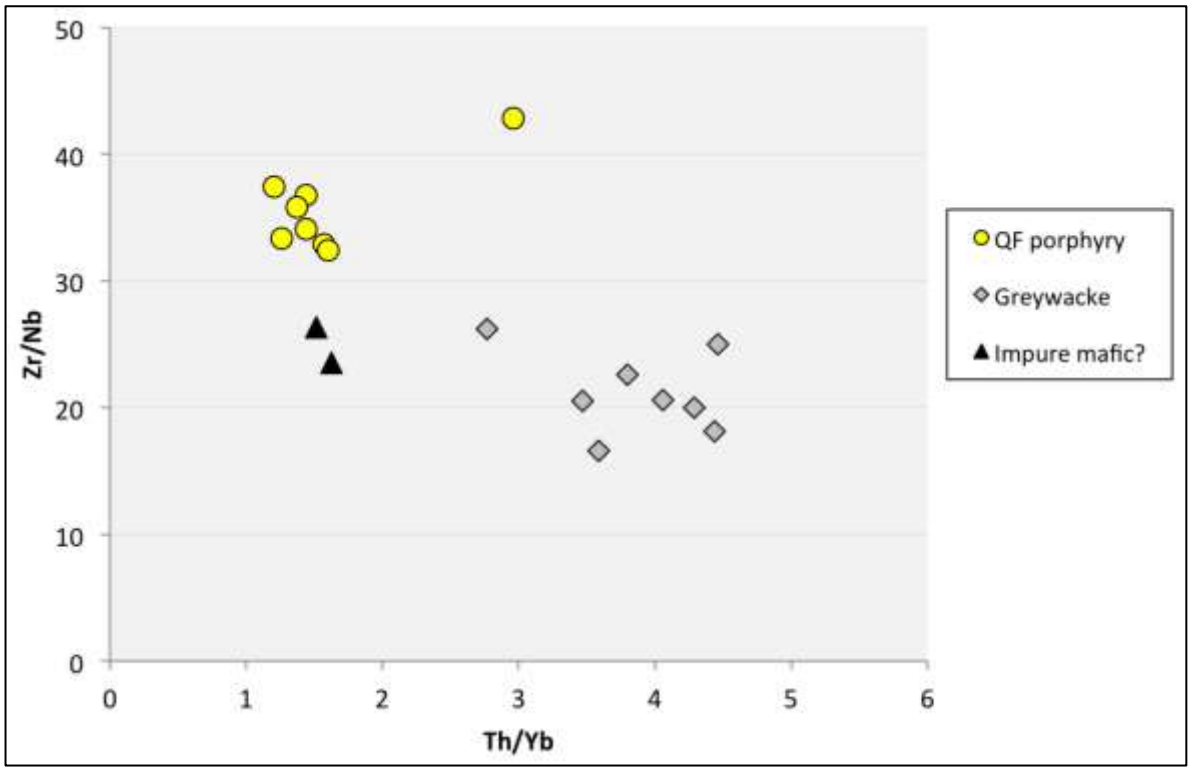
50
40
30
20
10
0
Zr/Nb
0
1
2
3
4
5
6
Th/Yb
QF porphyry
Greywacke
Impure mafic?

Figure 4 (cont).

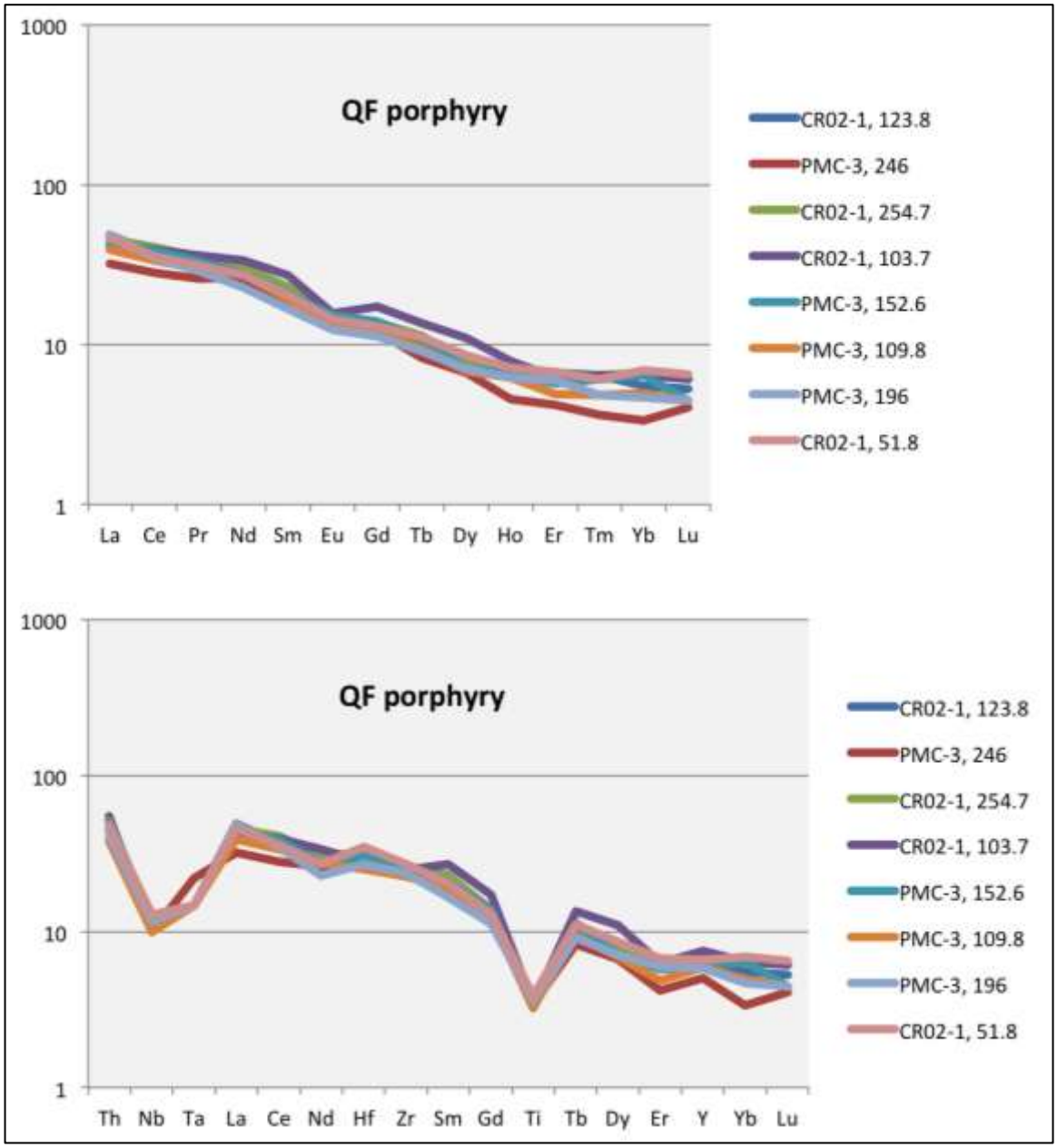

Figure 5a. REE (upper) and extended incompatible-element (lower) plots for the Carr QF porphyry. The slope of the patterns together with the negative Nb-Ta anomalies indicate that the magmas have a calc-alkaline affinity and were probably formed in a subduction-related setting. All data normalized to the chondritic values of McDonough and Sun (1995).

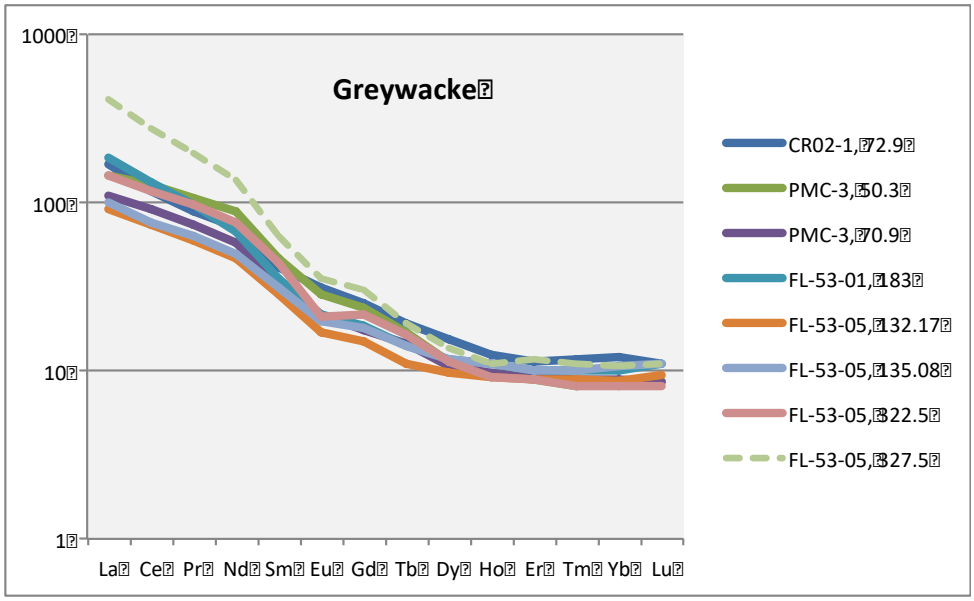

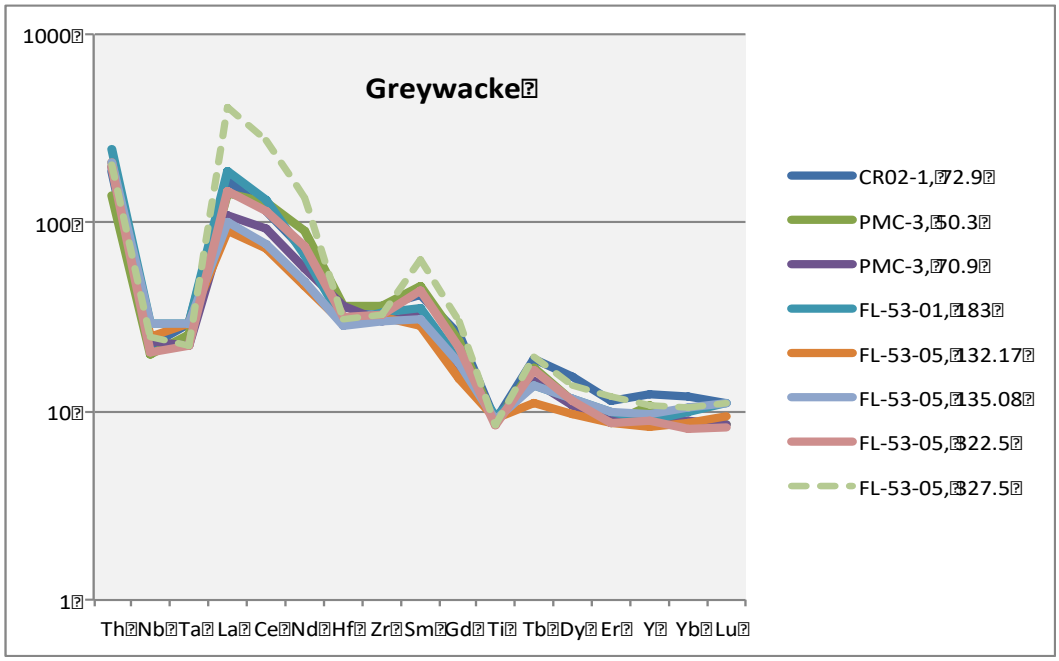

Figure 5b. REE (upper) and extended incompatible-element (lower) plots for greywackes flanking the margin of the Carr QF porphyry.

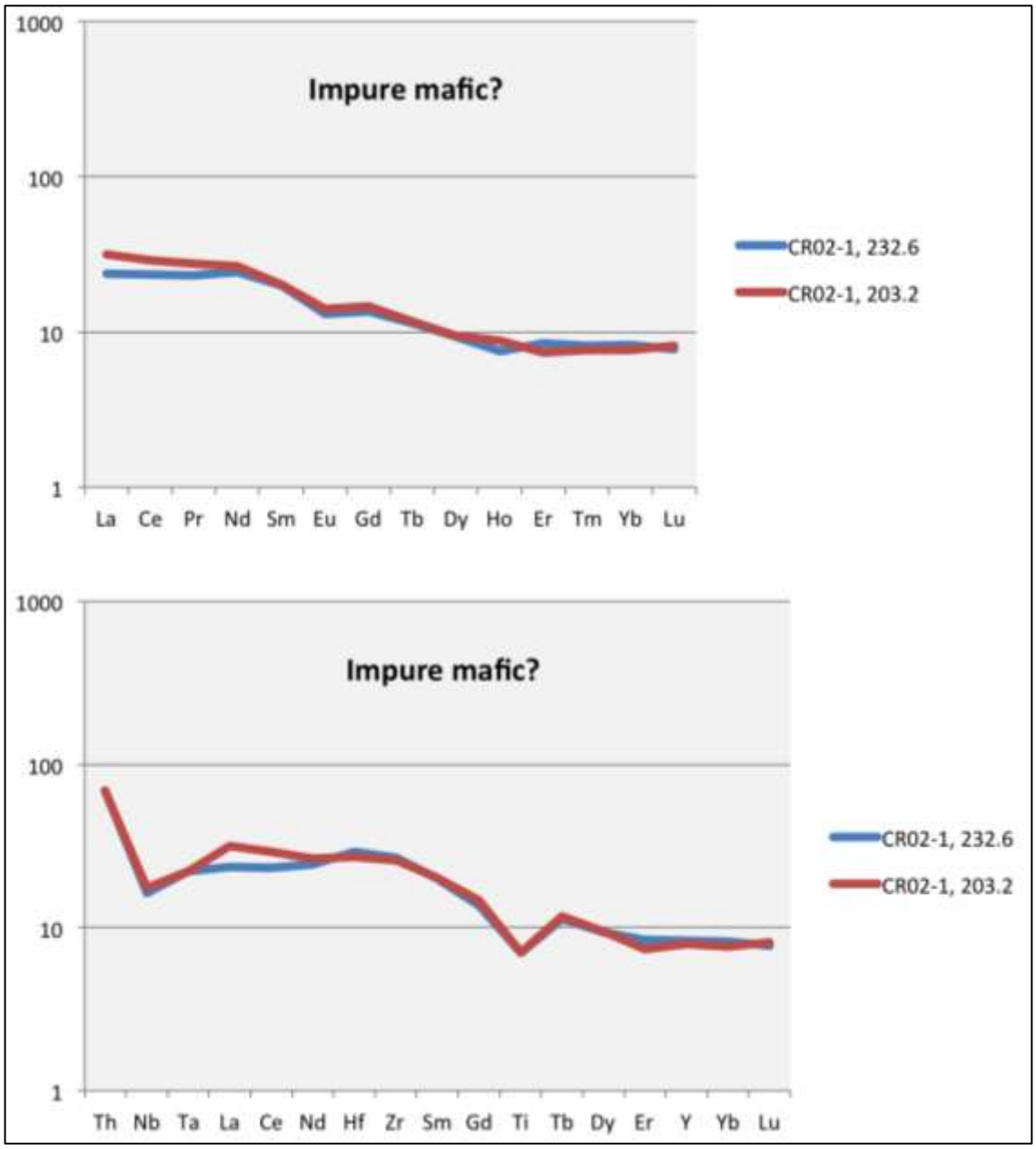

Figure 5c. REE (upper) and extended incompatible-element (lower) plots for a mafic hybrid? lithology of transitional affinity that flanks the Carr QF porphyry in drillhole CR02-1.

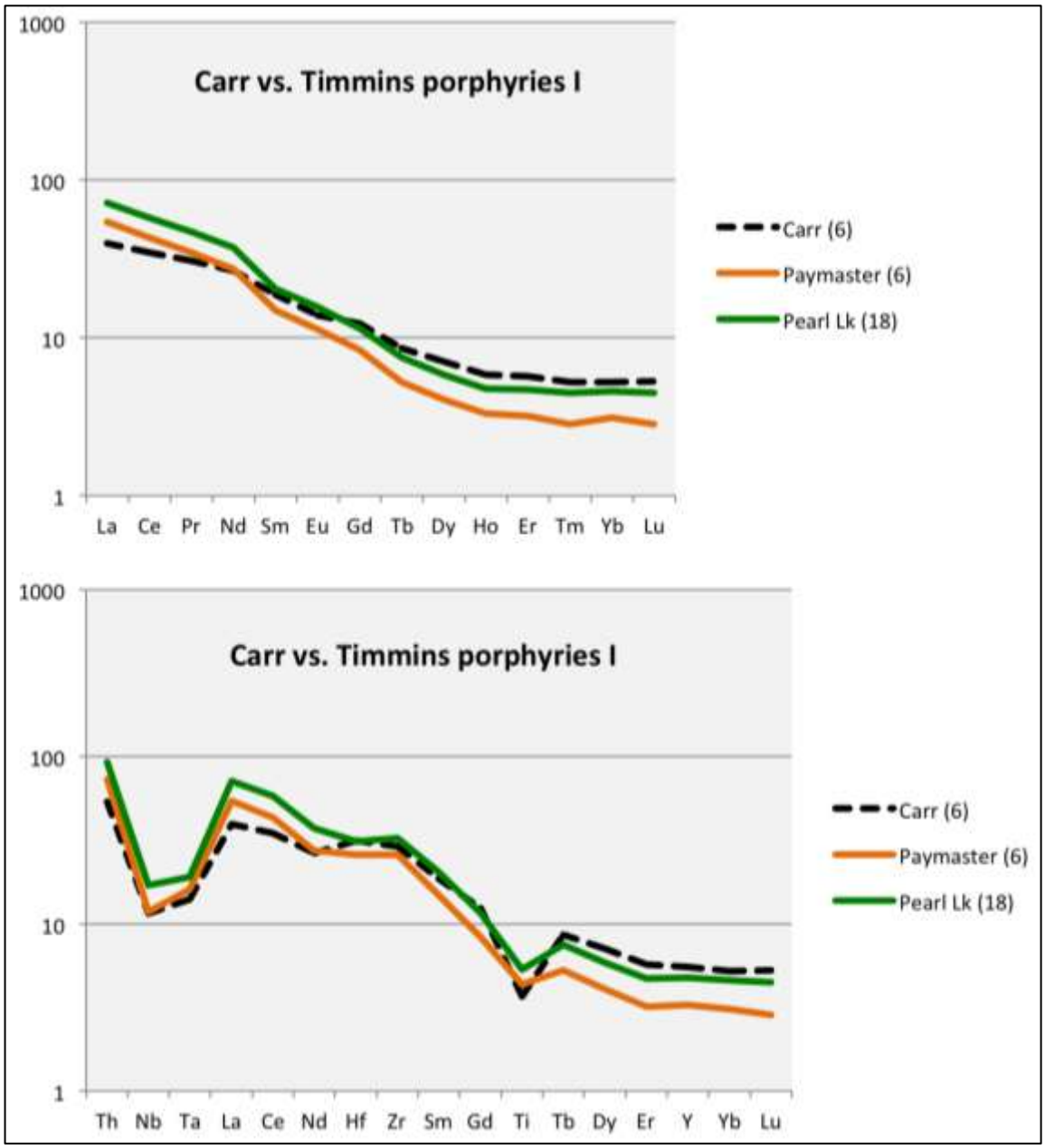

Figure 6a. REE (upper) and extended incompatible-element (lower) plots for the Carr QF porphyry (black dashed line) and the closely similar Paymaster and Pearl Lake porphyries in Timmins. All data from Macdonald (2005), normalized to the chondritic values of McDonough and Sun (1995).

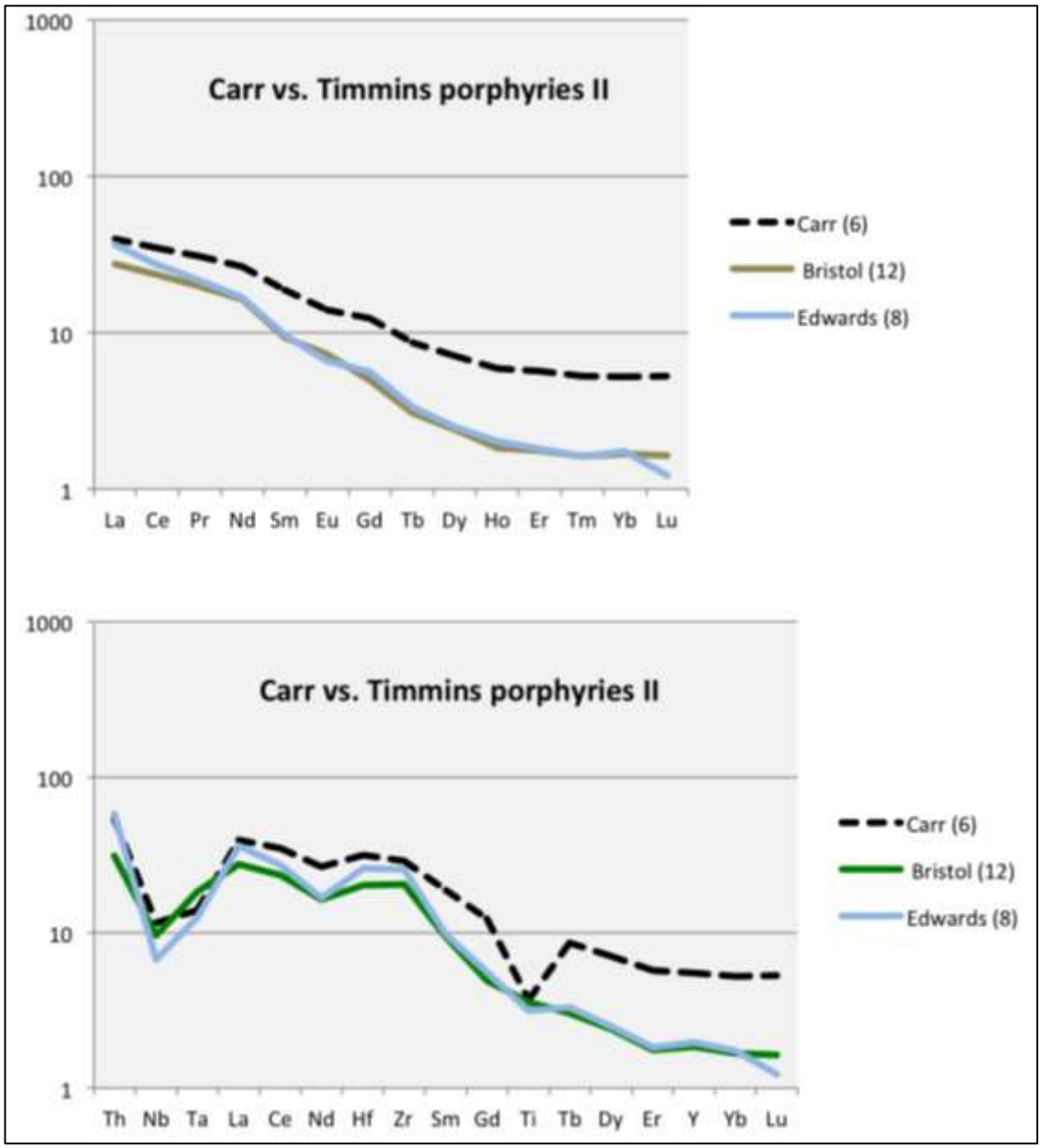

Figure 6b. Comparison of Carr QF porphyry (black dashed line) with the strongly calc-alkaline Bristol and Edwards porphyries of the Timmins area. All data from Macdonald (2005), normalized to the chondritic values of McDonough and Sun (1995).

As shown in Figures 4 and 5, and in Table 1, the Carr porphyry in PCM-3 and CR02-1 has a near-uniform composition, although petrographically it ranges from having subequal amounts of quartz and feldspar phenocrysts to being feldspar-dominated. The porphyry is sodic, with 5-7 % Na2O. On an LOI-free basis, SiO2 contents are about 70 %. These features indicate that the porphyry is best classified as a trondhjemite. It is chemically comparable to many of the sodic QF porphyries in the Timmins area. Many of these porphyries, for example, the Pearl Lake and Paymaster porphyries, are associated with major gold deposits. At the McIntyre mine, the Pearl Lake porphyry hosted Cu and Mo in addition to gold (Bateman et al., 2008). The Carr porphyry is notably less alkaline than the Bristol and Edwards porphyries.

Chemical alteration in the Carr porphyry samples appears to be limited, although mineralogical alteration is clearly visible in the drill core (mainly as several percent carbonate and variable amounts of sericite). The sericite generally does not appear to have resulted from addition of K to the porphyry, but from hydration of a minor primary K-bearing phase. An exception is sample CR02-1, 103.7m, where K has been added at the expense of Na and Ca. One sample (PCM-3, 109.8m) contains about 15 % carbonate, mainly as veins.

The greywackes have a near-uniform composition and are chemically almost unaltered, apart from sample PCM-3, 70.9m, where notable K has been added at the expense of Na. This sample is however very low in total sulfur and metals. By contrast, a greywacke from FL-53-05, 327.5m contains 1.05 % Cu and 0.39 ppm Au. Interestingly, this sample is chemically almost unaltered, apart from the addition of 2.1 % sulfur and a small decrease in silica.

The dark rock that is adjacent to some of the porphyry units in hole CR02-1 is provisionally interpreted as a hybrid lithology resulting from contamination of a mafic magma due to assimilation of a small amount of QF porphyry. The two samples of mafic hybrid rock that were taken do not appear to be chemically altered and contain no metal enrichments.

Four of the 8 samples of QF porphyry in the new data set contain 1000-3000 ppm Cu, while four of the 8 greywacke samples contain 800-2000 ppm Cu, with one sample (noted above) containing 10,500 ppm Cu. Gold contents range from 10-100 ppb, with one sample (noted above) containing 387 ppb Au. Three samples of QF porphyry also contain 0.01 % Mo.

Hole PMC-3

Downhole plots of several chemical parameters for hole PCM-3 are given in Figure 7, together with the main logged units. Photographs of the litho samples and other features of interest are given in Figure 8 to 15. The sequence in this hole is very simple, with a greywacke interval followed downhole by QF porphyry, in which the hole ended. Four samples of the QF porphyry show little downhole variation, with SiO2 values in the high 60s and about 2 % MgO and 6 % Na2O. The overall chemistry is equivalent to that of a rhyodacite. Of the four samples of QF porphyry, the sample at 196.0m was the most mineralized (0.71 % S, 0.30 % Cu and 0.01 % Mo). In this sample, pyrite + chalcopyrite occur in fine veinlets (Fig. 14).

Hole CR02-1

Downhole plots of various chemical parameters for hole CR02-1 are shown in Figure 16, with drill core and thin-section photographs given in Figures 17 to 30. The sequence of lithologies in this hole is more complex than in PCM-3, presumably due to the presence of thin dykes or sills of porphyry near the margin of the main mass of Carr porphyry. In addition, an unusual lithology is present in the lower part of the hole, between intervals of porphyry, that has some chemical features of a mafic rock, yet carries scattered quartz and plagioclase phenocrysts up to 5 mm across. This lithology, termed a hybrid mafic, is tentatively interpreted to have resulted from intrusion of a mafic magma (of unknown age) near the contact between the Carr porphyry and greywackes to the north, with some assimilation of material from the Carr porphyry. Of the 8 whole-rock samples, a greywacke at 72.9m contains 0.57 % S and 0.16 % Cu, while a porphyry at 254.7m contains 0.62 % S, 0.09 % Cu, and 0.01 % Mo.

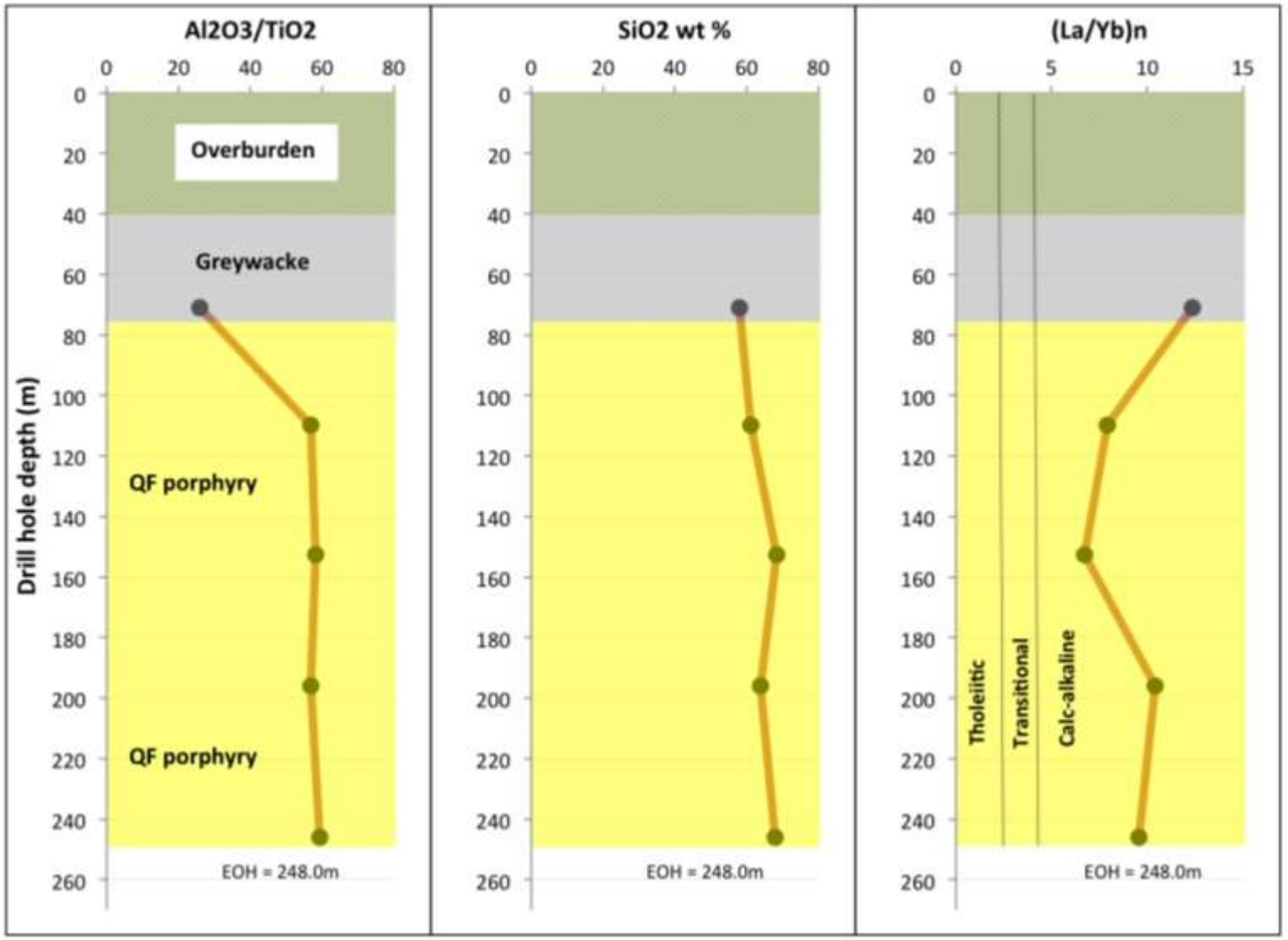

Fig. 7. Downhole plots of Al2O3/TiO2 (primary composition), SiO2, and La/Yb (affinity) for whole-rock samples from hole PCM-3.

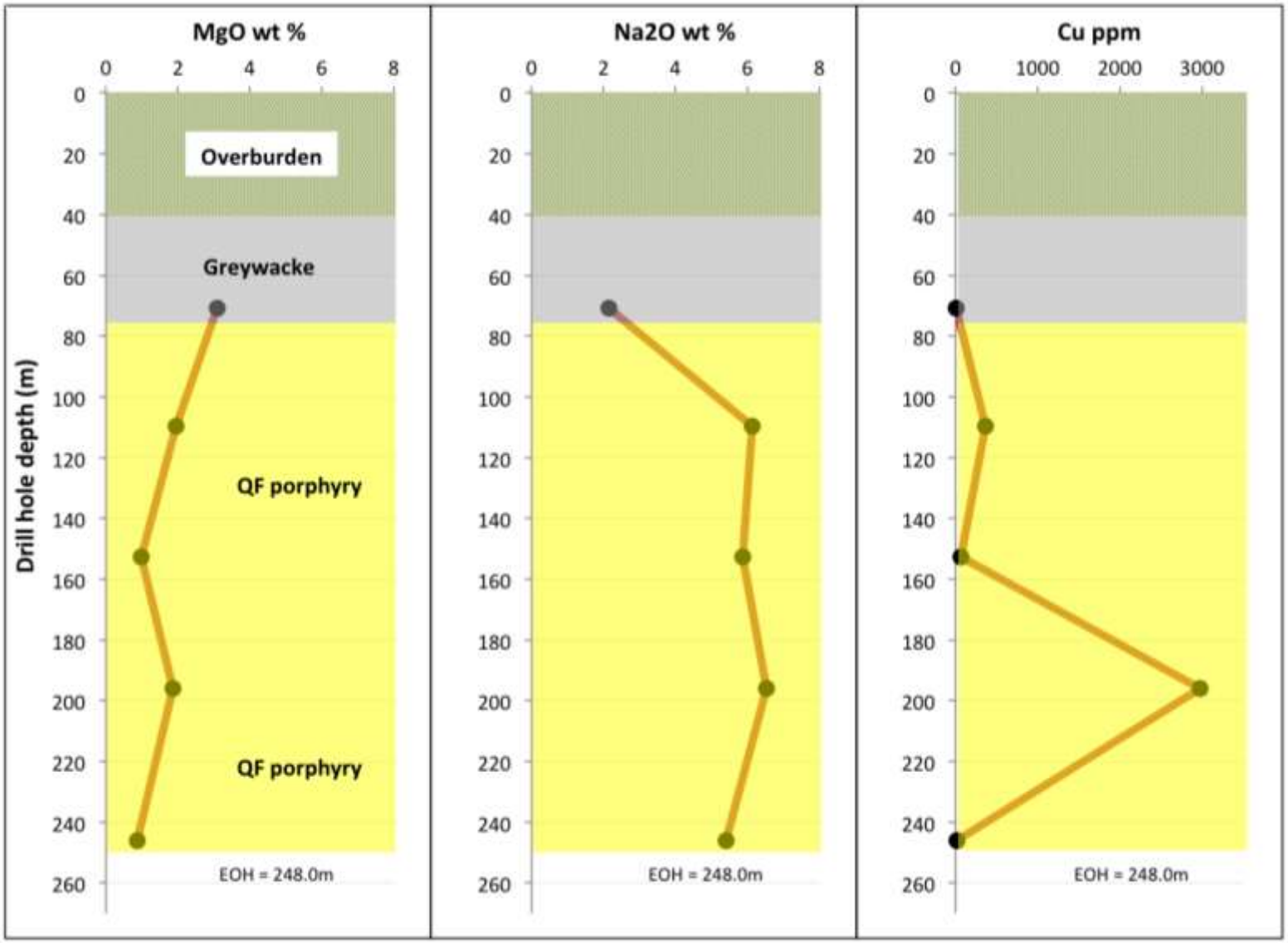

Fig. 7 (cont). Downhole plots of MgO, Na2O and Cu for whole-rock samples from hole PCM-3. The QF porphyry is strongly sodic.

Fig. 8a. PMC-3, 50.3m. Litho sample of greywacke (at flagging) taken by Berger (2000).

Fig. 8b. PMC-3. Greywacke – QF porphyry contact at 73.2m (arrow). Litho sample of greywacke at 70.9m shows addition of K.

Fig. 9a. PMC-3, 109.8m. Litho sample of QF porphyry. The paler areas are due to increased amounts of fine-grained carbonate. Petro sample at 111.4m (see below).

Fig. 9b. PMC-3, 111.4m. QF porphyry. Phenocrysts mainly plagioclase of various sizes, some cut by sericite-carbonate shears. Quartz phenos are small and minor. Crossed polars. Width of view = 5 mm.

Fig. 10a. PMC-3. Pinky-beige-altered QF porphyry with carbonate-chlorite vein at 139.0m (arrow).

Fig. 10b. PMC-3, 139.0m. Petro sample of carbonate-chlorite vein in QF porphyry (see Fig. 11).

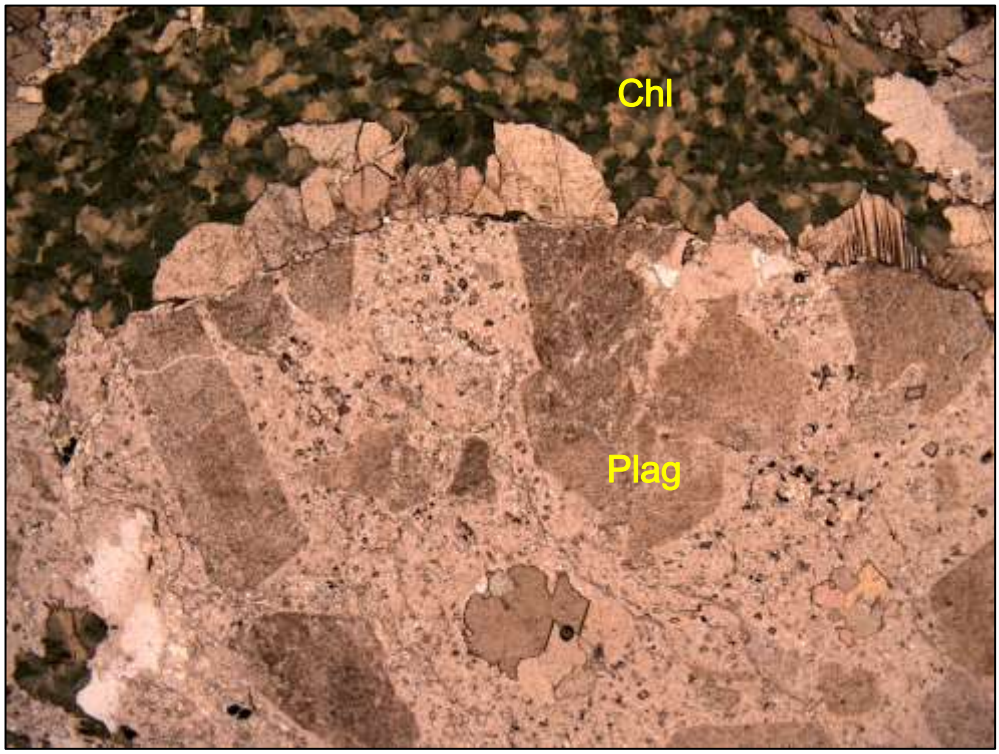

Fig. 11a. PMC-3, 139.0m. Vein of khaki-coloured chlorite cutting feldspar porphyry. Plane light, width of view = 5 mm.

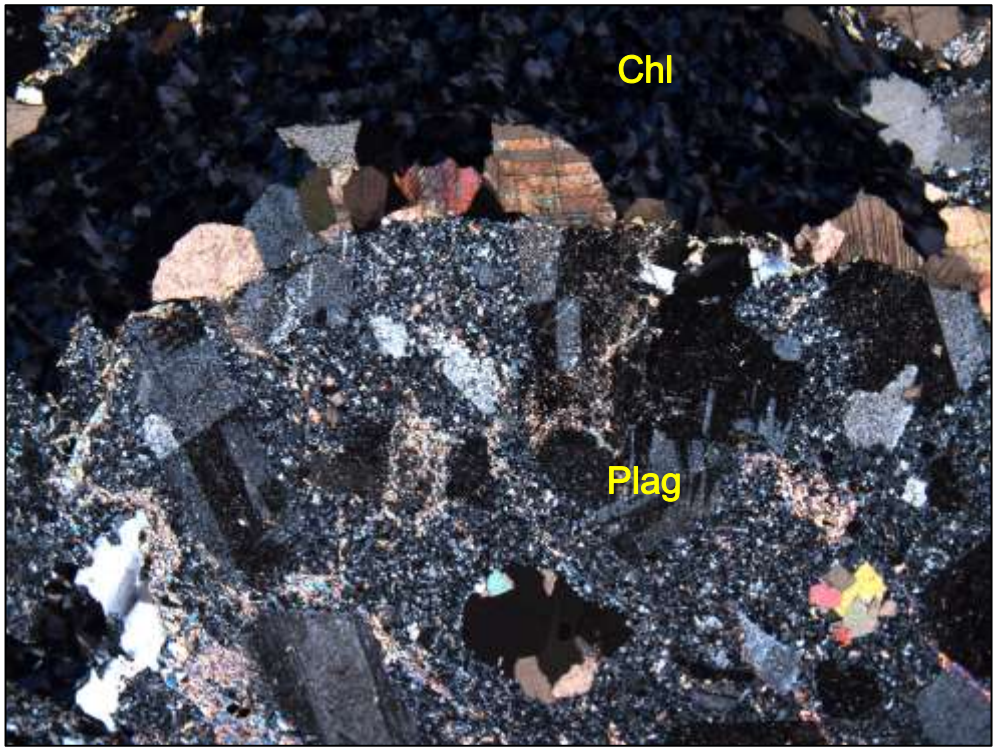

Fig. 11b. Same view as above, but in crossed polars. Bluish birefringence of chlorite suggests it is iron-rich. Carbonate occurs along vein margin. Phenocrysts in the host rock are mainly plagioclase.

Fig. 12a. PMC-3, 152.6m. Litho sample of QF porphyry.

Fig. 12b. PMC-3, 195.0m. Litho sample of QF porphyry cut by sulfide veinlets. Sample contain 6.5 % Na2O, 0.71 % S, 0.30 % Cu and 0.01 % Mo. Petro sample at 194.8m (see Fig. 13).

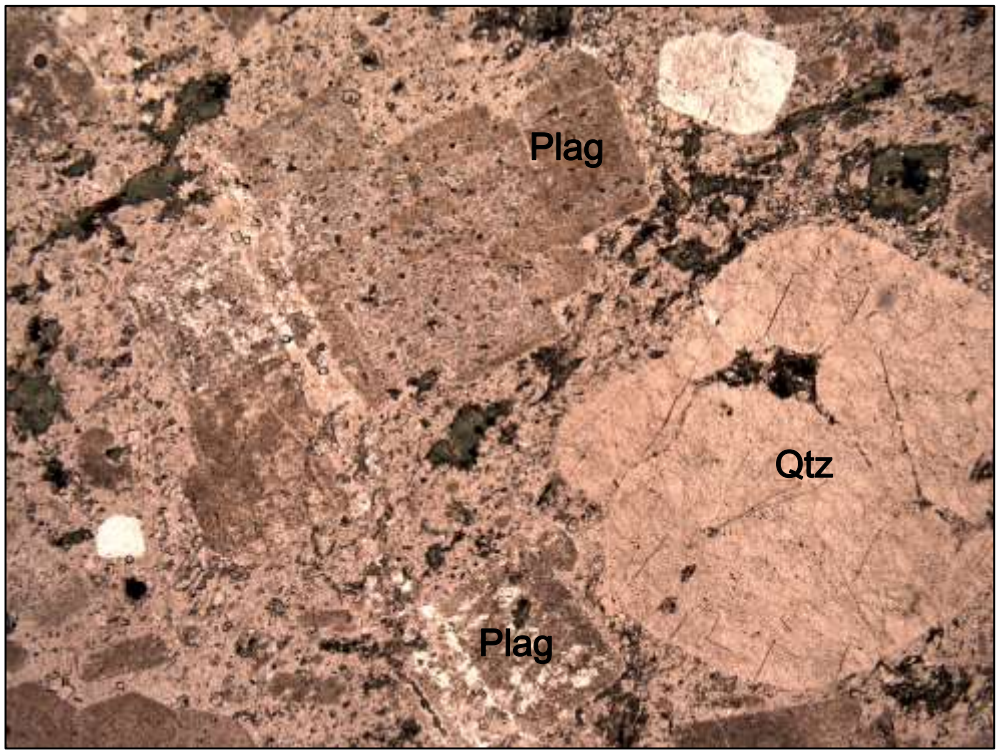

Fig. 13a. PMC-3, 194.8m. QF porphyry. Plane light, width of view = 5 mm.

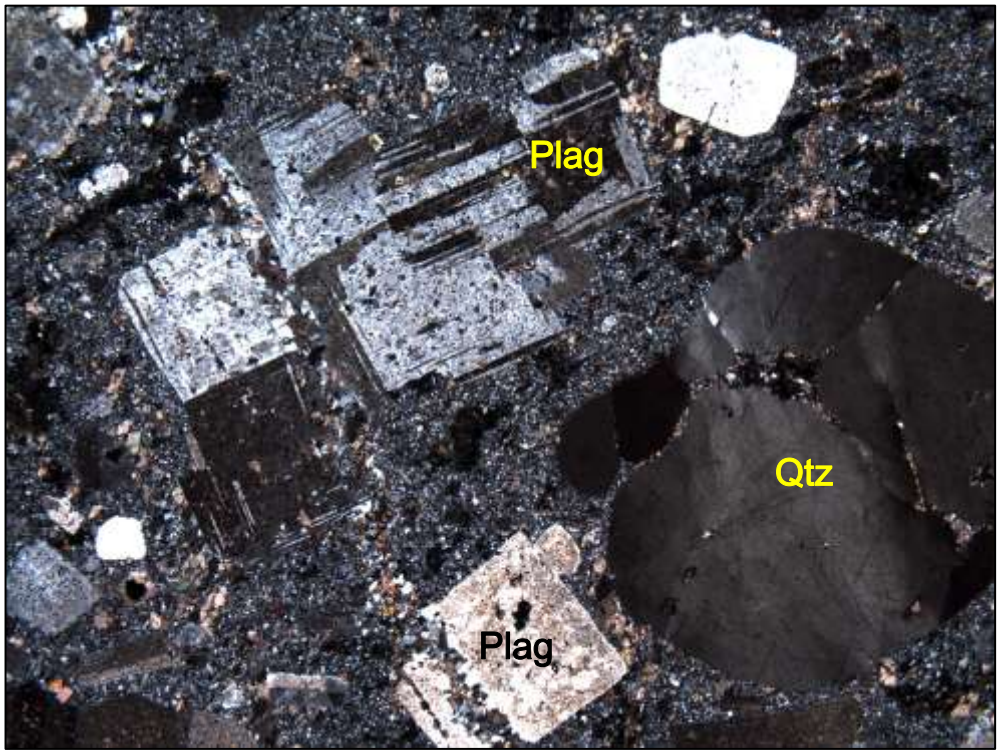

Fig. 13b. Same view as above, but in crossed polars. Note general lack of alteration.

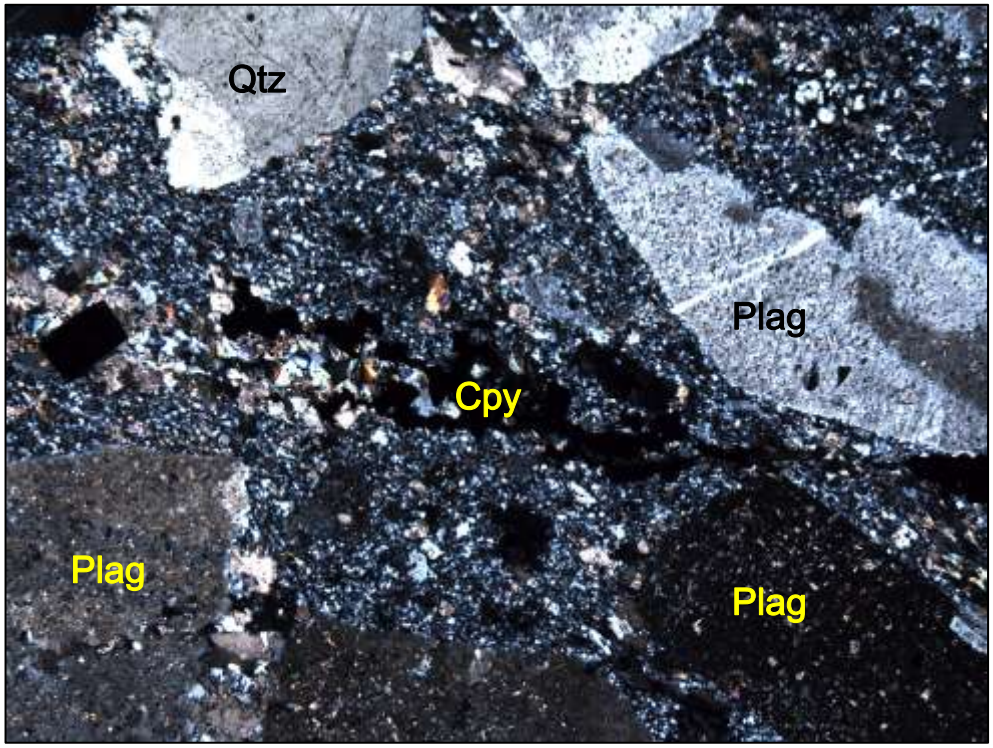

Fig. 14a. PMC-3, 194.8m. QF porphyry with sulfide veinlet (opaque) cutting matrix. Sample contains minor chlorite, sericite and carbonate in microseams. Crossed polars, width of view = 2.5 mm.

Fig. 14b. Same view as above, but in reflected light, showing veinlet of chalcopyrite and 1 pyrite grain.

Fig. 15. PMC-3, 195.0m. Litho sample of QF porphyry.

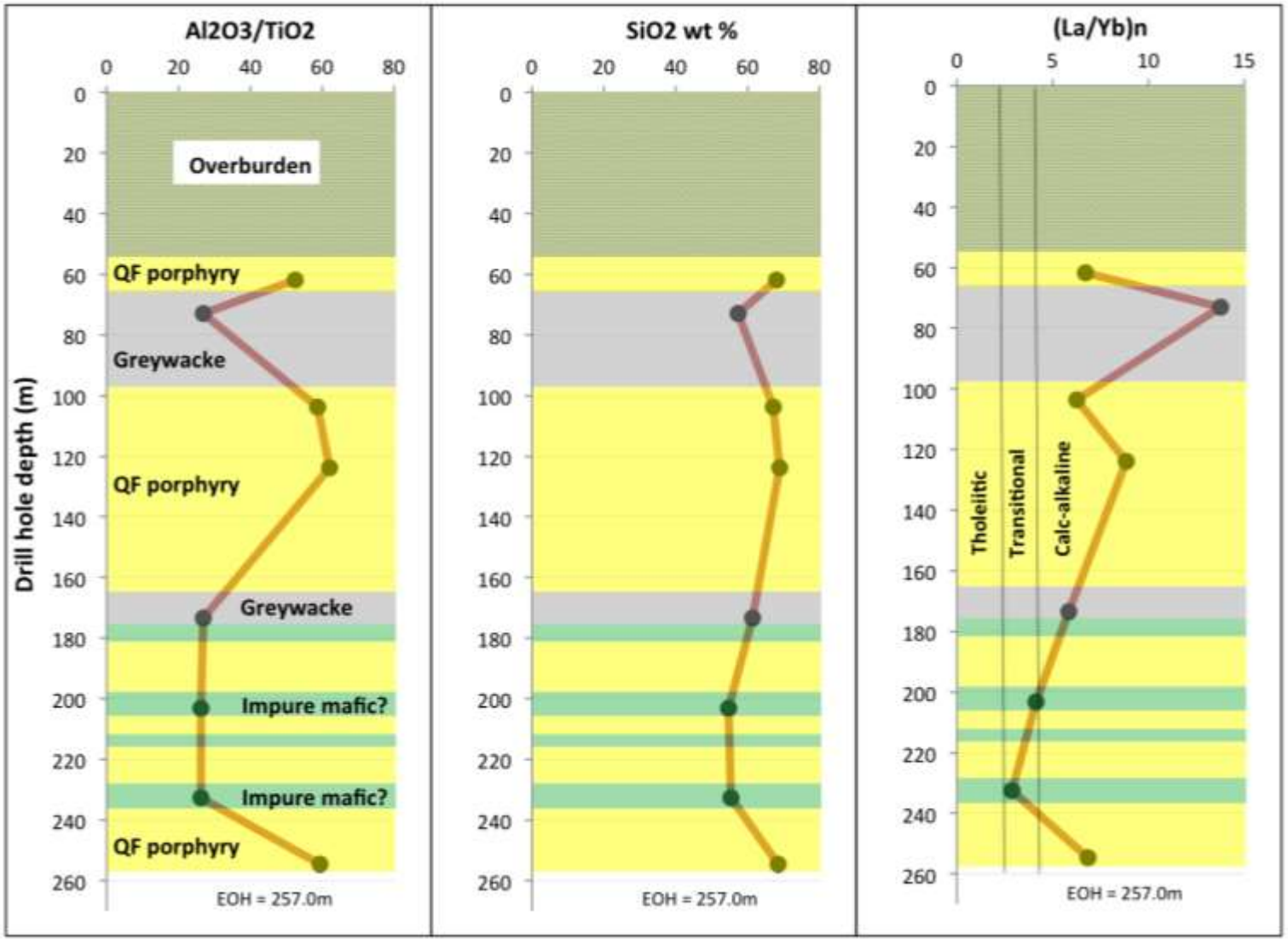

Fig. 16. Downhole plots of Al2O3/TiO2 (primary composition), SiO2, and La/Yb (affinity) for whole-rock samples from hole CR02-1.

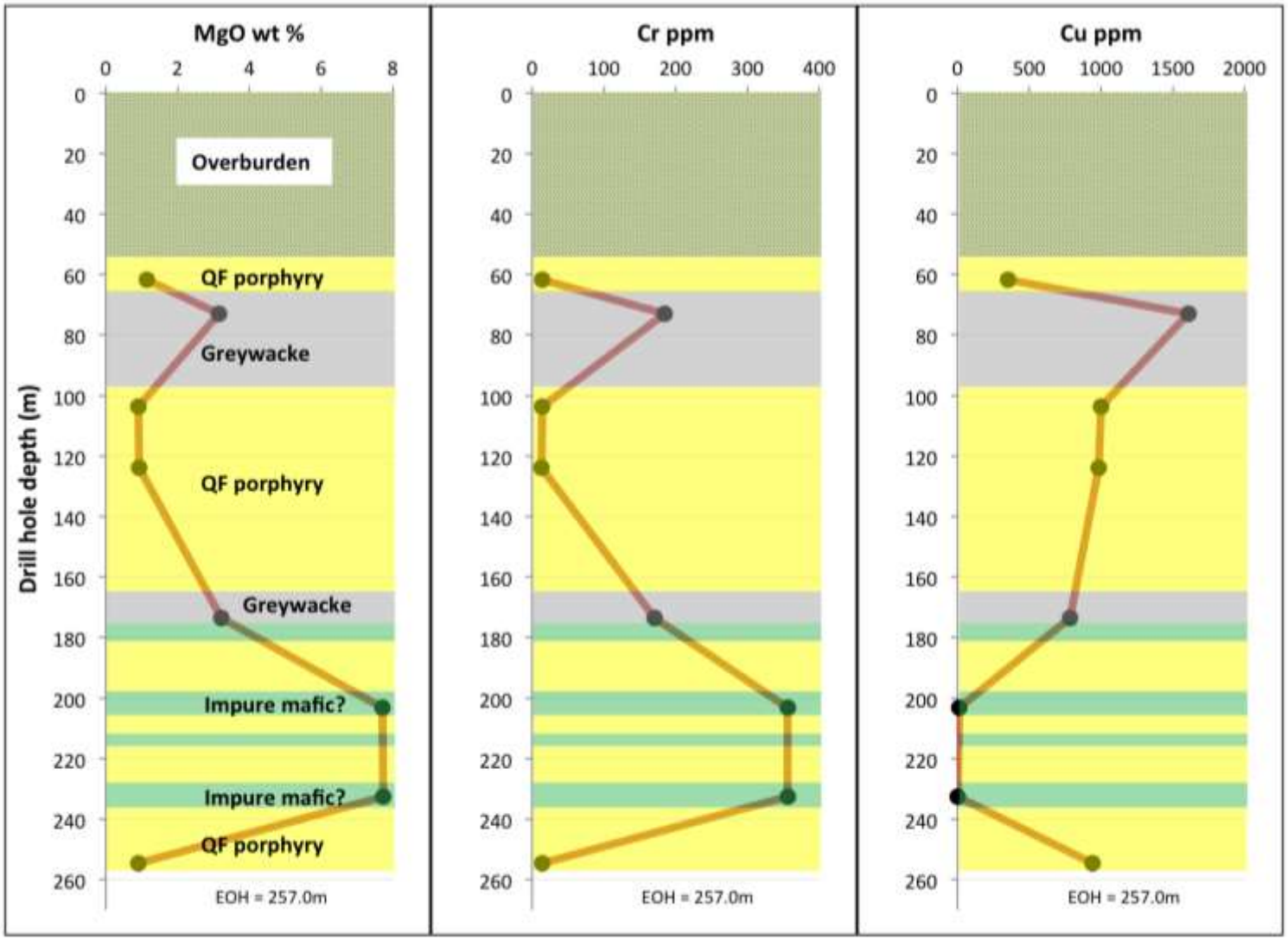

Fig. 16 (cont). Downhole plots of MgO, Cr and Cu for whole-rock samples from hole CR02-1. The mafic? Lithology has rather high Mg and Cr contents. Cu enrichments (500-1500 ppm) occur in both the QF porphyry and the greywacke.

Fig. 17a. CR02-1, 56.9m. Petro sample of sulfide-veined and altered QF porphyry.

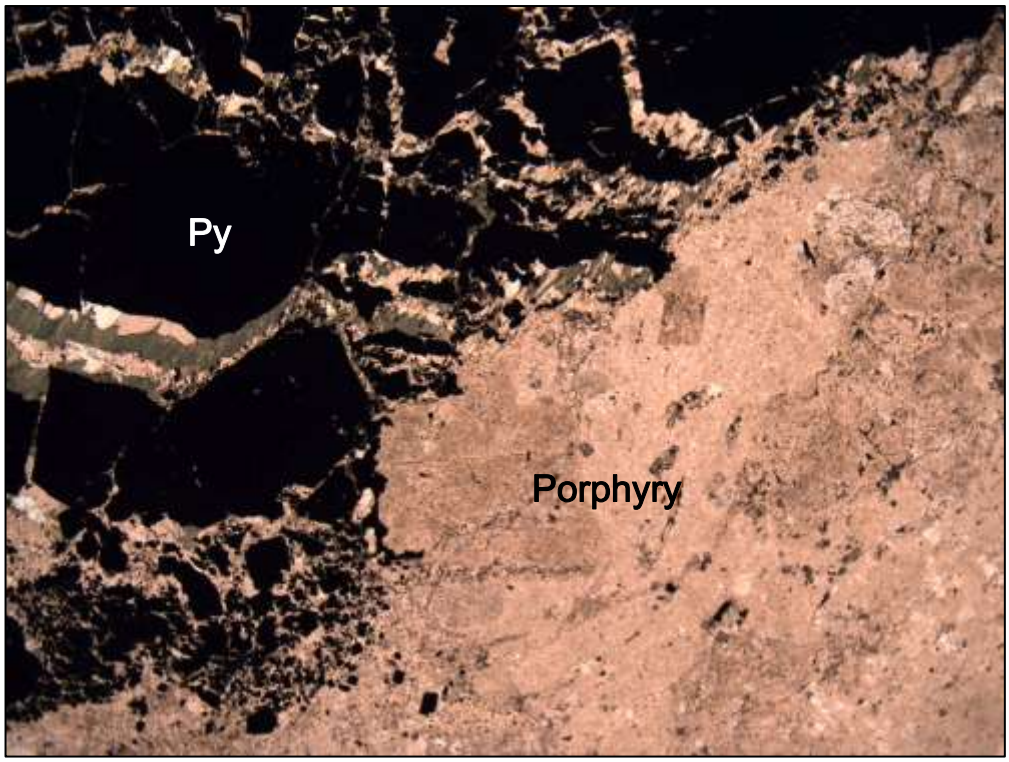

Fig. 17b. CR02-1, 56.9m, QF porphyry cut by sulfide clot. Plane light, width of view = 5 mm.

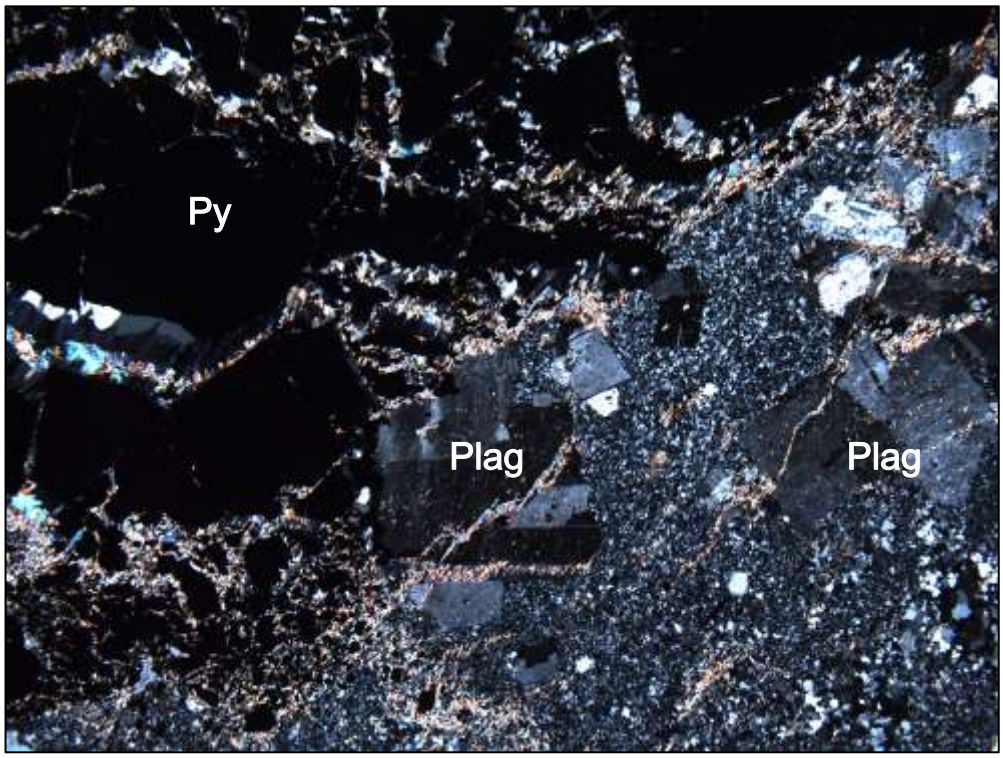

Fig. 18a. QF porphyry cut by fractured sulfide mass, which in turn is cut by sericite ± chlorite ±quartz microveinlets. Phenocrysts are mainly plagioclase. Crossed polars, width of view = 5 mm.

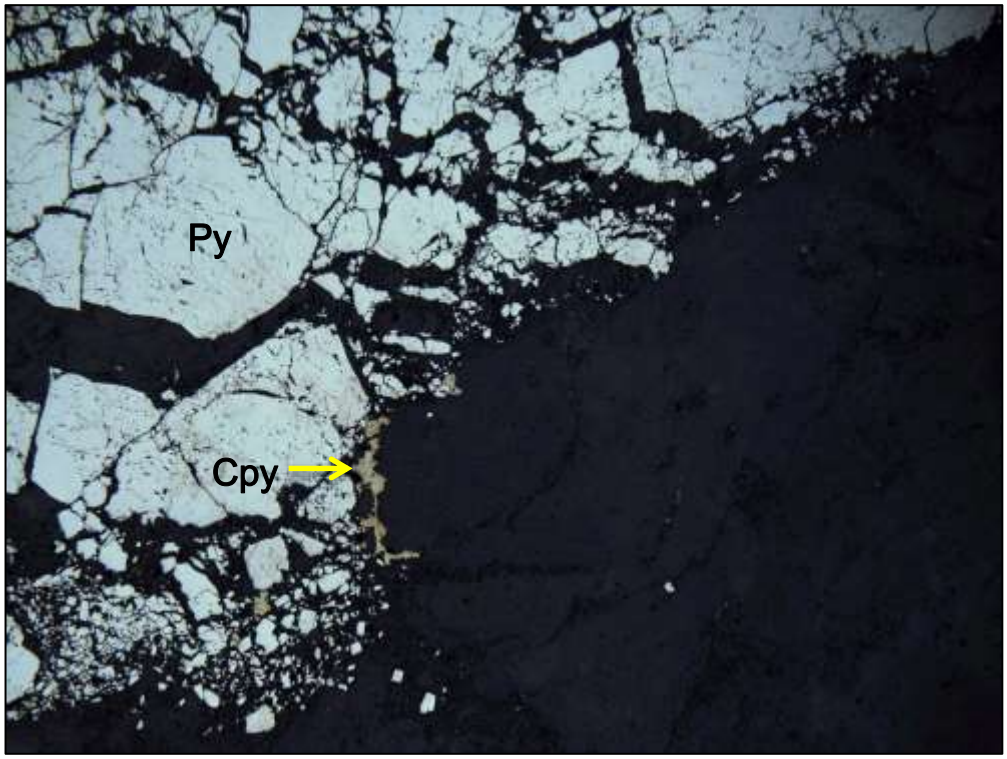

Fig. 18b. Same view as above, but in reflected light. Main mass of sulfide is pyrite, with minor chalcopyrite between the pyrite and the host porphyry.

Fig. 19a. CR02-1, 61.8m. Litho sample of QF porphyry.

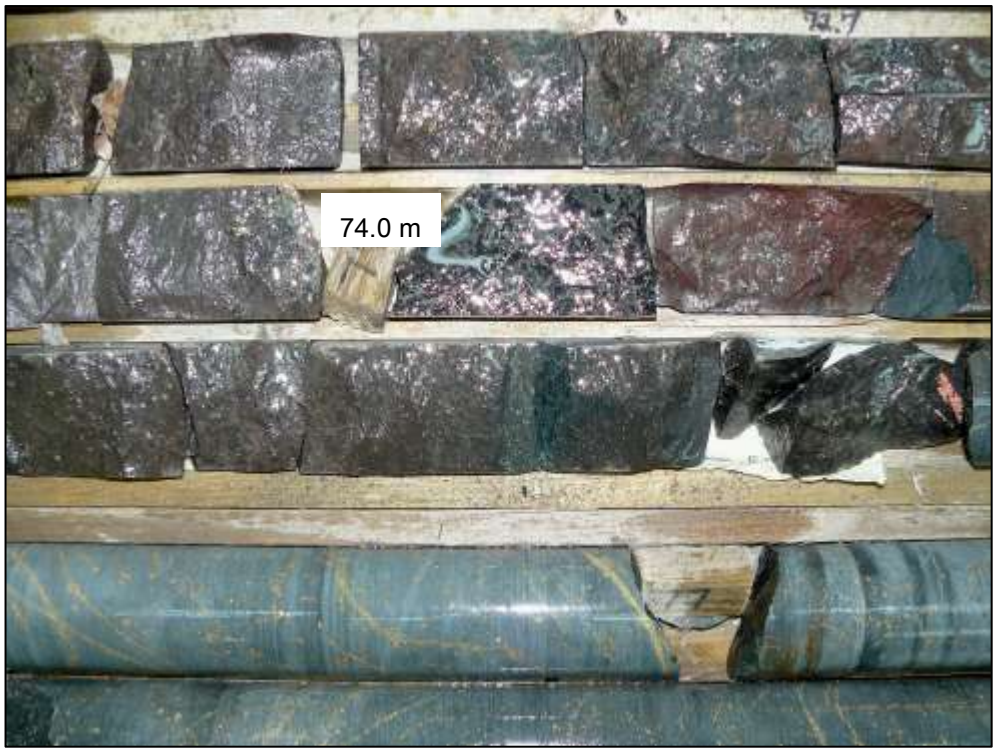

Fig. 19b. CR02-1, 72.5-77.1m. Litho sample of greywacke at 72.9m (just to right of top slot). Sample contains 0.57 % S and 0.16 % Cu. Despite the reddish tinge, the greywacke contains 6.8 % Na2O.

Fig. 20a. CR02-1, 72.6m. Petro sample of fine greywacke (see Fig. 21).

Fig. 20b. CR02-1, 87.5-89.0m. Faint bedding in greywacke (arrow). Spots are carbonate rhombs.

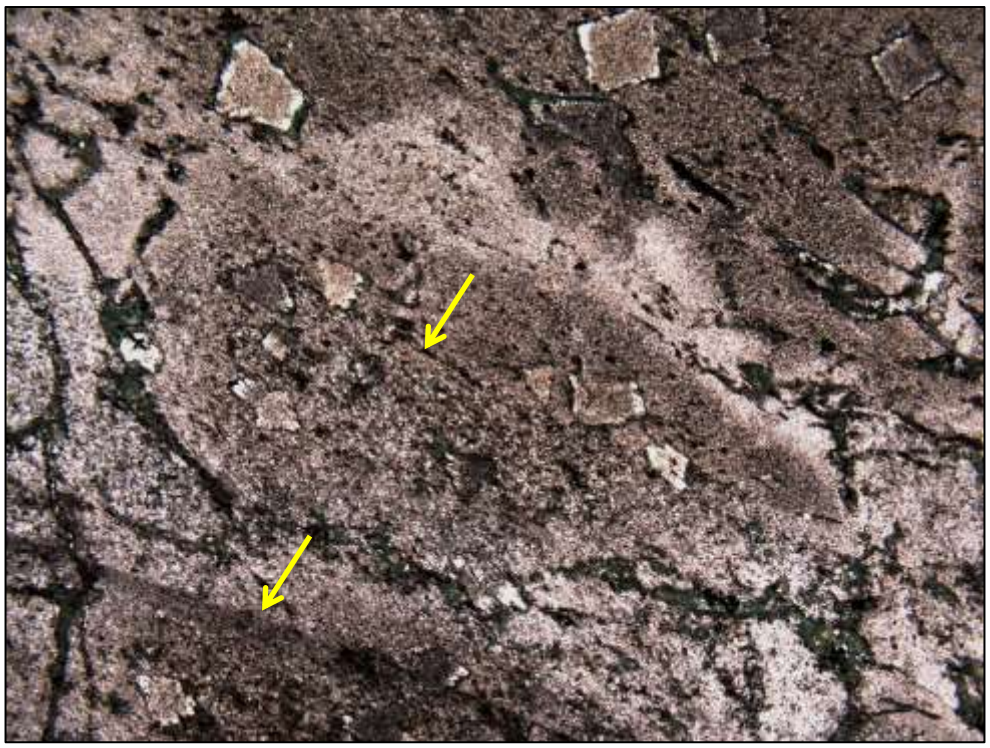

Fig. 21a. CR02-1, 72.6m. Siltstone with scattered carbonate rhombs. Plane light, width of view = 5 mm. Margins of fine sand bed marked by arrows. Microveinlets contain chlorite + sulfide.

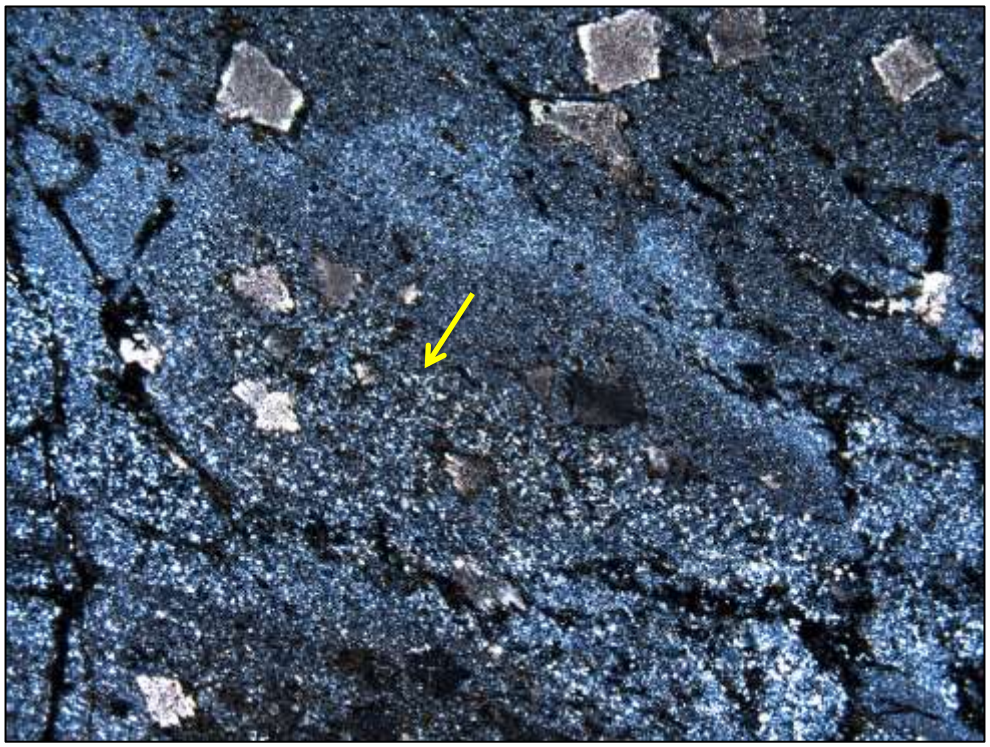

Fig. 21b. Same view as above, but in crossed polars.

Fig. 22a. CR02-1. Sharp contact between greywacke and QF porphyry at 98.7m.

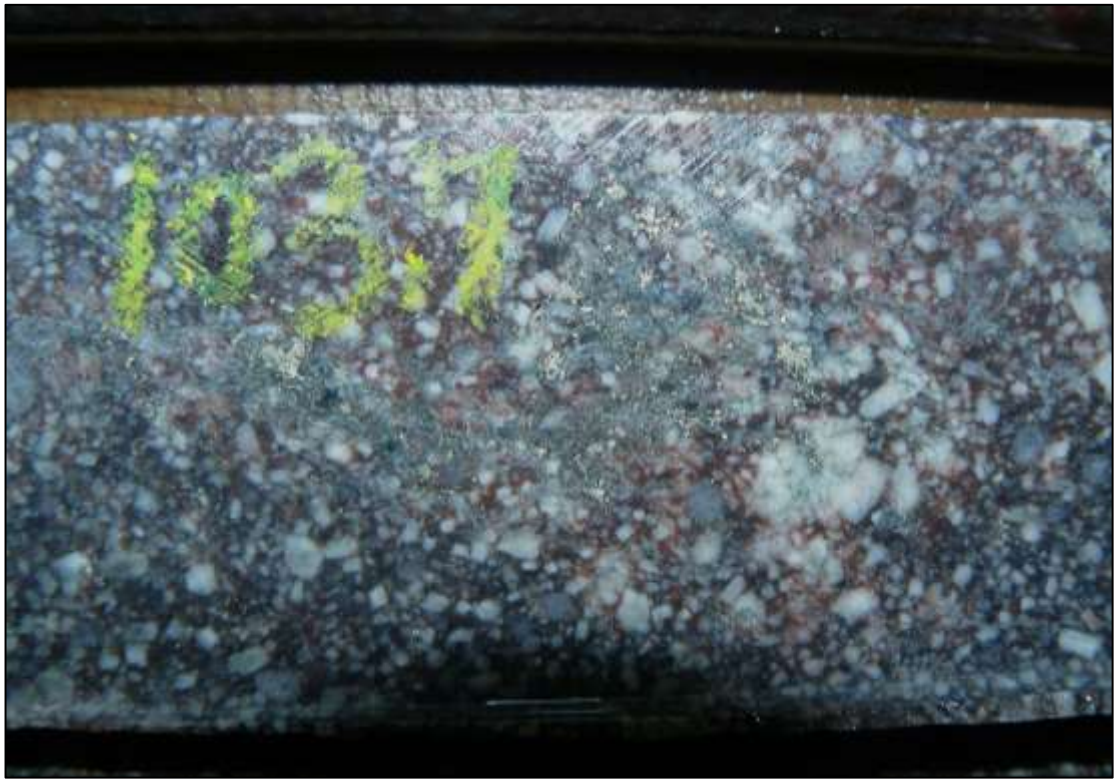

Fig. 22b. CR02-1, 103.7m. Litho sample QF porphyry at 103.7m. A high K2O content of 5.0 % suggests that K has been added during alteration. Sample also contains 0.10 % Cu.

Fig. 23a. CR02-1, 123.8m. Litho sample of mineralogically altered QF porphyry (quartered core at 123.6-124.0m). Chemically, the rock is little modified, although it contains 0.23 % S and 0.10 % Cu.

Fig. 23b. CR02-1, 123.0m. Petro sample of sulfide-veined QF porphyry (see Fig. 24).

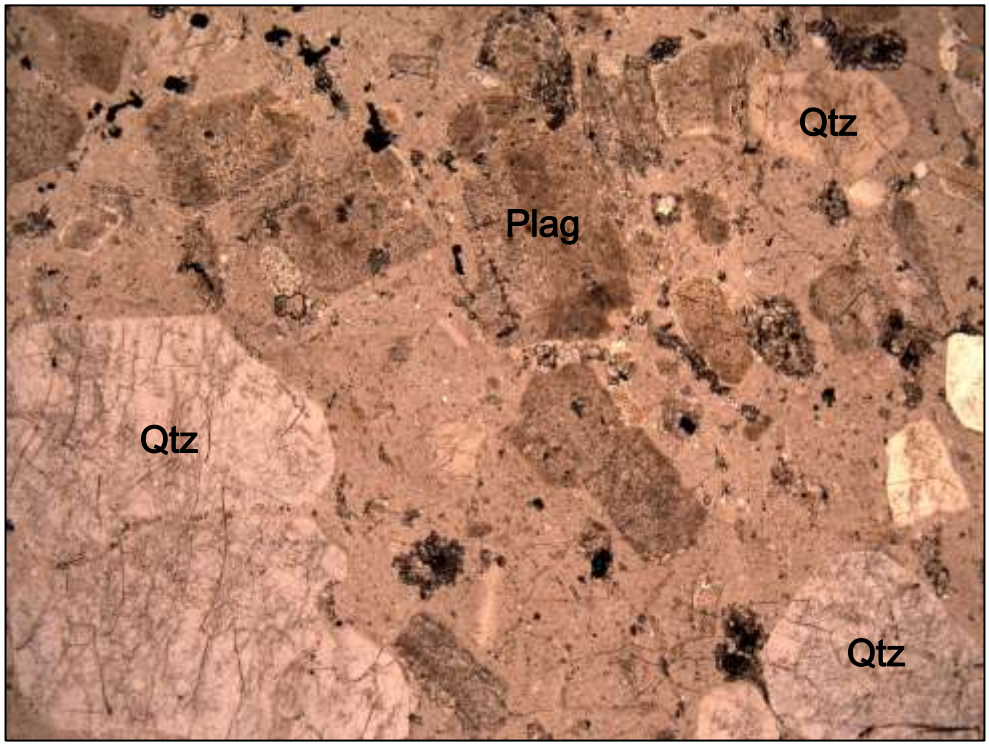

Fig. 24a. CR02-1, 123.0m. QF porphyry. Large quartz and smaller plagioclase phenocrysts. Plane light, width of view = 5 mm.

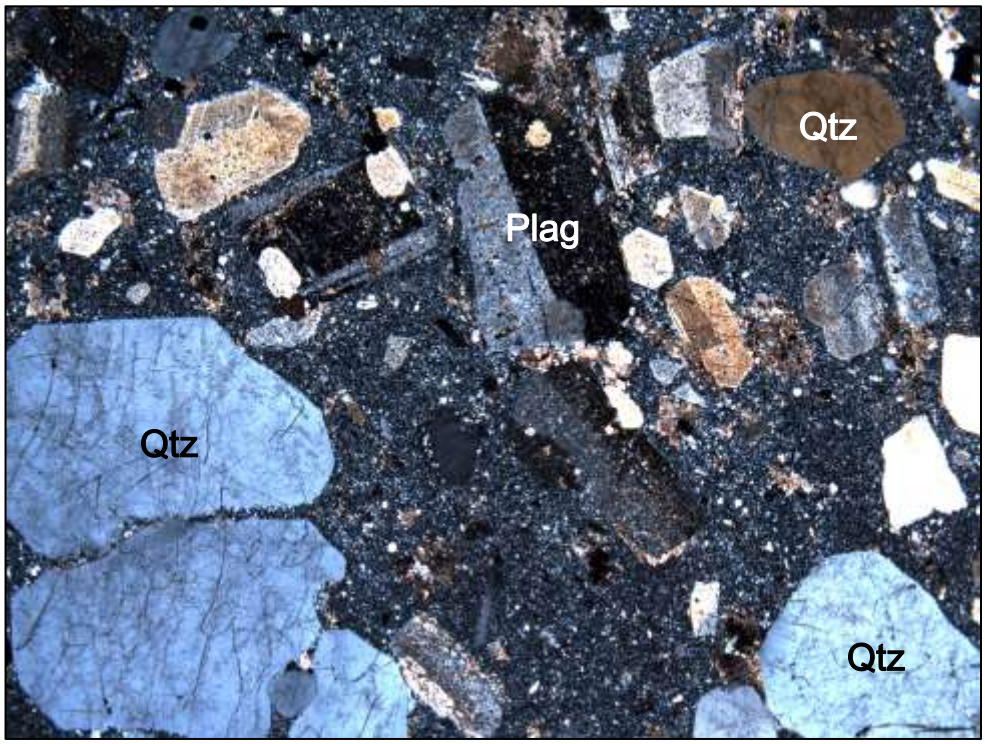

Fig. 24b. Same view as above, but in crossed polars. Little alteration is evident.

Fig. 25a. CR02-1, 165.6m. Contact between QF porphyry and fine greywacke.

Fig. 25b. CR02-1, 173.5m. Litho sample of fine greywacke. Sample contains 0.23 % S and 0.08 % Cu.

Fig. 26a. CR02-1. Contact at 180.7m (marked) between impure mafic rock and QF porphyry.

Fig. 26b. CR02-1. QF porphyry and impure mafic rock (contact is at 198.1m, just out of view). Note scattered phenocrysts of quartz and feldspar in the mafic rock.

Fig. 27a. CR02-1, 203.2m. Litho sample of impure mafic rock. Although this lithology carries large quartz grains, it is has the Mg and Cr contents of a mafic rock. The quartz grains may be xenocrysts.

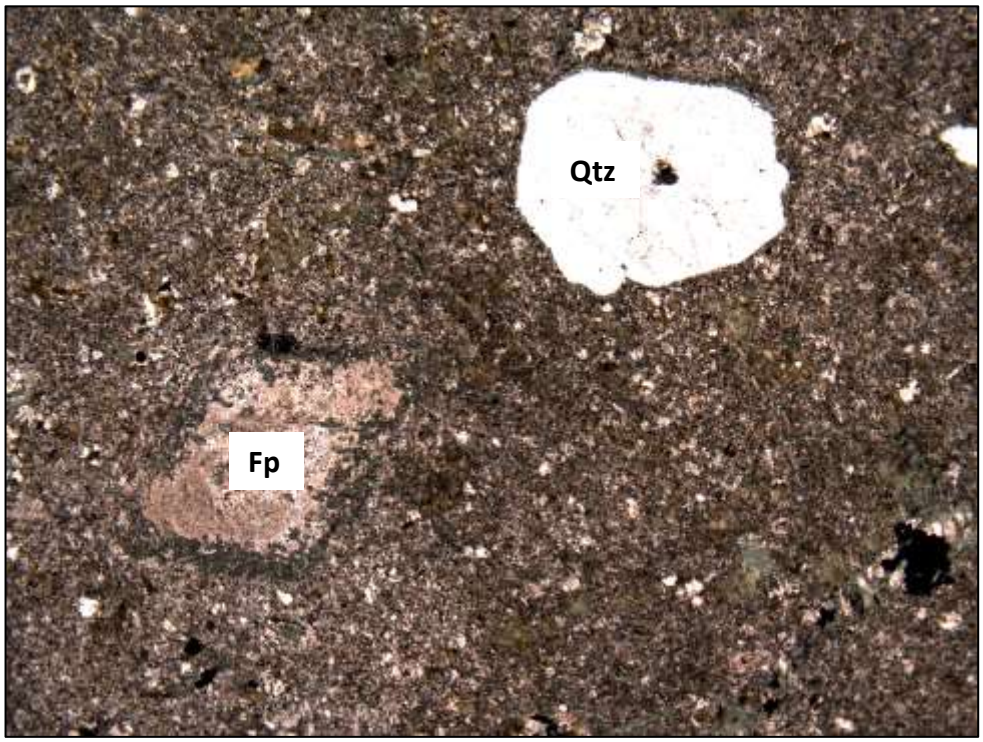

Fig. 27b. CR02-1, 203.3m (core photo above). Quartz grain and altered feldspar grain in “mafic” matrix containing fine chlorite and phlogopite. Plane light, width of view = 5 mm.

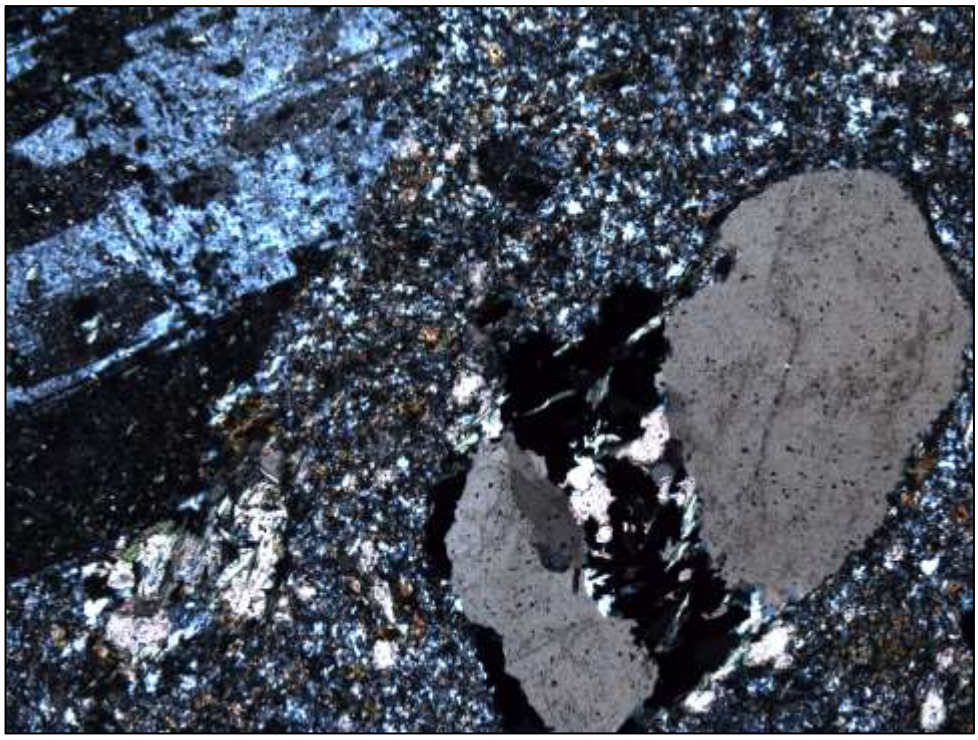

Fig. 28a. CR02-1, 203.3m (see Fig. 27a). Large plagioclase and quartz grains in “mafic” matrix. Quartz grain is cut by sulfides. Plagioclase and quartz may be xenocrysts. Crossed polars, width = 2.5 mm.

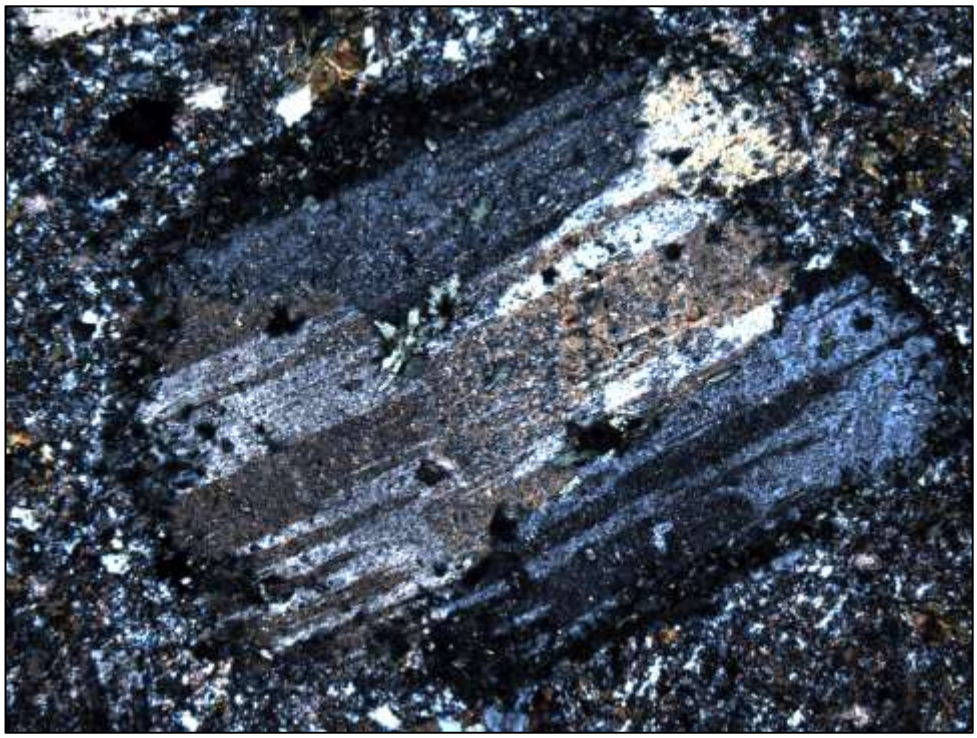

Fig. 28b. CR02-1, 203.3m. Plagioclase grain with chloritic rim in “mafic” matrix. Rim is interpreted as a reaction zone between mafic magma and a plagioclase xenocryst. Crossed polars, width = 2.5 mm.

Fig. 29a. CR02-1. QF porphyry and impure mafic rock. Contact is at 228.9m (not in view).

Fig. 29b. CR02-1. Litho sample at 232.6m of impure mafic rock. Note large quartz grains.

Fig. 30a. CR02-1, 240.4-243.5m. QF porphyry, with sulfides in fractures below 242.0m.

Fig. 30b. CR02-1, 254.7m. Litho sample of QF porphyry with 7.1 % Na2O, 0.62 % S and 0.09 % Cu.

References

Ayer, J.A., Amelin, Y., Corfu, F., Kamo, S.L., Ketchum, J.W.F., Kwok, K. and Trowell, N., 2002. Evolution of the southern Abitibi greenstone belt based on U-Pb geochronology: autochthonous volcanic construction followed by plutonism, regional deformation and sedimentation. Precambrian Research, v. 115, p. 63-95.

Ayer, J.A., Goutier, J., Thurston, P.C., Dubé, B., and Kamber, B.S., 2010. Tectonic and metallogenic evolution of the Abitibi and Wawa subprovinces. Summary of Field Work and Other Activities 2010, Ontario Geological Survey, Open File Report 6260, p. 3-1 to 3-6.

Barrett, T.J., MacLean, W.H. and Årebäck, H., 2005. The Palaeoproterozoic Kristineberg VMS deposit, Skellefte district, northern Sweden. Part II: chemostratigraphy and alteration. *Mineralium Deposita*, v. 40, p. 368-395.

Barrett, T.J., MacLean, W.H. and Tennant, S.C., 2001. Volcanic sequence and alteration at the Parys Mountain volcanic-hosted massive sulfide deposit, Wales, United Kingdom: applications of immobile element lithogeochemistry. *Economic Geology*, v. 96, p. 1279-1305.

Barrett, T.J. and MacLean, W.H., 1999. Volcanic sequences, lithogeochemistry, and hydrothermal alteration in some bimodal volcanic-associated massive sulfide systems. In: Volcanic-Associated Massive Sulfide Systems: Processes and Examples in Modern and Ancient Settings (C.T. Barrie and M.D. Hannington, editors). Reviews in Economic Geology, Volume 8, p. 101-131.

Barrett, T.J. and MacLean, W.H., 1991. Chemical, mass, and oxygen-isotopic changes during extreme hydrothermal alteration of an Archean rhyolite, Noranda. Economic Geology, v. 86, p. 406-414.

Bateman, R., Ayer, J.A. and Dubé, B., 2008. The Timmins-Porcupine gold camp, Ontario: Anatomy of an Archean greenstone belt and ontogeny of gold mineralization. Economic Geology, v. 103, p. 1285-1308.

Berger, B.R., 2000. Geology of the Monteith area. Ontario Geological Survey, Open File Report 6024, pp. 77 + map foldout.

Dubé, B., and Gosselin, P., 2007, Greenstone-hosted quartz-carbonate vein deposits. In: Goodfellow, W.D., ed., Mineral Deposits of Canada. Geological Association of Canada, Mineral Deposits Division, Special Publication No. 5, p. 49-73.

Ispolatov, V., Lafrance, B., Dubé, B., Creaser, R.A., and Hamilton, M., 2008. Geologic and structural setting of gold mineralization in the Kirkland Lake-Larder Lake gold belt, Ontario. Economic Geology, v. 103, p. 1309-1340.

MacLean, W.H. and Barrett, T.J., 1993. Lithogeochemical methods using immobile elements. Journal of Exploration Geochemistry, v. 48, p. 109-133.

MacLean, W.H. and Kranidiotis, P., 1987. Immobile elements as monitors of mass transfer in hydrothermal alteration: Phelps Dodge massive sulphide deposit, Matagami, Quebec. Economic Geology, v. 82, p. 951-962.

MacDonald, P.J., 2010. The geology, lithogeochemistry and petrogenesis of intrusions associated with gold mineralization in the Porcupine gold camp, Timmins, Canada. MSc thesis, Laurentian University, Sudbury, Ontario, pp. 188.

MacDonald, P.J., Piercey, S.J. and Hamilton, M.A., 2005. An integrated study of intrusive rocks spatially associated with gold and base metal mineralization in the Abitibi greenstone belt, Timmins area and Clifford Township: Discover Abitibi Initiative. Ontario Geological Survey, Open File Report 6160, pp. 189.

McDonough, W.F. and Sun, S-s., 1995. The composition of the Earth. Chemical Geology, v. 120, p. 223-253.

Scott Wilson Roscoe Postle Associates, 2006. Technical report on the Taylor, Clavos, Hislop and Stock projects in the Timmins area, northeastern Ontario, Canada. Prepared for St Andrew Goldfields Ltd., by W.E. Roscoe and N.N. Gow, pp. 163.